

JAERI-Review

98-012



**THE PREMIXING AND PROPAGATION PHASES OF FUEL-COOLANT
INTERACTIONS: A REVIEW OF RECENT EXPERIMENTAL
STUDIES AND CODE DEVELOPMENTS**

September 1998

**Anhar Riza ANTARIKSAWAN*, Kiyofumi MORIYAMA, Hyun-sun PARK,
Yu MARUYAMA, Yanhura YANG and Jun SUGIMOTO**

**日本原子力研究所
Japan Atomic Energy Research Institute**

本レポートは、日本原子力研究所が不定期に公開している研究報告書です。

入手の間合わせは、日本原子力研究所研究情報部研究情報課（〒319-1195 茨城県那珂郡東海村）あて、お申し越してください。なお、このほかに財団法人原子力弘済会資料センター（〒319-1195 茨城県那珂郡東海村日本原子力研究所内）で複写による実費領布をおこなっております。

This report is issued irregularly.

Inquiries about availability of the reports should be addressed to Research Information Division, Department of Intellectual Resources, Japan Atomic Energy Research Institute, Tokai-mura, Naka-gun, Ibarakiken 319-1195, Japan.

**The Premixing and Propagation Phases of Fuel-coolant Interactions:
A Review of Recent Experimental Studies and Code Developments**

**Anhar Riza ANTARIKSAWAN*, Kiyofumi MORIYAMA, Hyun-sun PARK,
Yu MARUYAMA, Yanhua YANG* and Jun SUGIMOTO**

**Department of Reactor Safety Research
Nuclear Safety Research Center
Tokai Research Establishment
Japan Atomic Energy Research Institute
Tokai-mura, Naka-gun, Ibaraki-ken**

(Received August 18, 1998)

A vapor explosion (or an energetic fuel-coolant interactions, FCIs) is a process in which hot liquid (fuel) transfers its internal energy to colder, more volatile liquid (coolant) ; thus the coolant vaporizes at high pressure and expands and does works on its surroundings. Traditionally, the energetic fuel-coolant interactions could be distinguished in subsequent stages : premixing (or coarse mixing), triggering, propagation and expansion.

Realizing that better and realistic prediction of fuel-coolant interaction consequences will be available understanding the phenomenology in the premixing and propagation stages, many experimental and analytical studies have been performed during more than two decades. A lot of important achievements are obtained during the time. However, some fundamental aspects are still not clear enough ; thus the works are directed to that direction. In conjunction, the model/code development is pursuit. This is aimed to provide a scaling tool to bridge the experimental results to the real geometries, e.g. reactor pressure vessel, reactor containment.

The present review intends to collect the available information on the recent works performed to study the premixing and propagation phases.

Keywords : Vapor Explosion, FCI, Premixing, Propagation, Experiment, Model, Codes, Jet Breakup, Droplets Fragmentation

※ Domestic Research Fellow

* Reactor Safety Technology Research Center of BATAN, Indonesia

溶融燃料－冷却材相互作用における粗混合および伝播過程
－最近の実験および解析コード開発に関するレビュー－

日本原子力研究所安全性試験研究センター原子炉安全工学部
Anhar Riza ANTARIKSAWAN*・森山 清史・Hyun-sun PARK
丸山 結・Yanhua YANG*・杉本 純

(1998年8月18日受理)

蒸気爆発（あるいは激しい燃料－冷却材相互作用、FCI）とは、高温液体（燃料）が低温の揮発性液体（冷却材）にその内部エネルギーを与え、低温液が急速に蒸発して高圧を発生し、周囲に仕事を与える過程である。蒸気爆発は従来から4段階の過程、すなわち初期粗混合、トリガリング、伝播および膨張の過程から成ると考えられている。

初期粗混合と伝播過程の現象を理解することにより蒸気爆発の結果をより精度良く予測できるであろうとの期待のもとに、20年以上にわたって多くの実験および解析的な研究が行われている。しかし、いくつかの基礎的な問題が未だ解決されておらず、その方向に研究が継続されている。さらに、実験結果と実炉の圧力容器あるいは格納容器の体系における現象の予測との橋渡しを行うスケーリングツールとして、モデルおよび解析コードの開発が進められている。

本報告は、初期粗混合および伝播過程に関する最近の研究についての情報を収集したものである。

Contents

1. Introduction	1
2. Experimental Works	3
2.1 Premixing Studies	3
2.1.1 MAGICO Experiment	3
2.1.2 QUEOS Experiment	5
2.1.3 BILLEAU Experiment	6
2.1.4 MIXA Experiment	6
2.1.5 PREMIX Experiment	7
2.1.6 ALPHA Experiment	8
2.1.7 FARO Experiment	10
2.2 Propagation Studies	12
2.2.1 SIGMA Experiment	12
2.2.2 IKE Multi Jet Experiment	13
2.2.3 KROTOS Experiment	14
3. Codes/Model Developments	16
3.1 IFCI Code	16
3.2 TEXAS Code	17
3.3 CHYMES Code	19
3.4 PM-ALPHA Code	20
3.5 MC3D Code	20
3.6 JASMINE Code	22
3.7 VESUVIUS Code	23
3.8 THIRMAL-1 Code	23
3.9 IKEJET Code	24
3.10 COMETA Code	25
3.11 TRACER-II	26
3.12 IVA Code	27
3.13 CULDESAC Code	28
3.14 ESPROSE.m Code	29
4. Summary	30
5. Concluding Remarks	30
Acknowledgement	31
References	32

目 次

1. 序 論	1
2. 実 験	3
2.1 粗混合過程	3
2.1.1 MAGICO	3
2.1.2 QUEOS	5
2.1.3 BILLEAU	6
2.1.4 MIXA	6
2.1.5 PREMIX	7
2.1.6 ALPHA	8
2.1.7 FARO	10
2.2 伝播過程	12
2.2.1 SIGMA	12
2.2.2 IKE 多ジェット実験	13
2.2.3 KROTOS	14
3. 解析コード／モデル開発	16
3.1 IFCI	16
3.2 TEXAS	17
3.3 CHYMES	19
3.4 PM-ALPHA	20
3.5 MC3D	20
3.6 JASMINE	22
3.7 VESUVIUS	23
3.8 THIRMAL-1	23
3.9 IKEJET	24
3.10 COMETA	25
3.11 TRACER-II	26
3.12 IVA	27
3.13 CULDESAC	28
3.14 ESPROSE.m	29
4. ま と め	30
5. 結 論	30
謝 辞	31
参考文献	32

LIST OF TABLES

Table 1	Specifications of the cold runs
Table 2	Specification of the hot runs
Table 3	Conditions of the MAGICO-2000 cold runs 2D slab geometry
Table 4	Conditions of the MAGICO-2000 hot runs 2D slab geometry
Table 5	Initial conditions of QUEOS hot experiments
Table 6	Conditions of first test series of BILLEAU
Table 7	Experiment conditions and main results
Table 8	Test run conditions of ALPHA-MJB
Table 9	Main data of FARO tests
Table 10	Initial conditions and main test results of alumina test series
Table 11	Initial conditions and main results of corium test series
Table 12	Summary of the recent FCI experimental works
Table 13	Summary of the code overview

LIST OF FIGURES

- Figure 1 Schematic of MAGICO-2000 experimental facility
- Figure 2 MAGICO-2000 experiments: superposition of X-ray radiographs and calculation results on jet contours
- Figure 3 QUEOS test facility
- Figure 4 QUEOS test: photograph of one cold run
- Figure 5 BILLEAU experiments: photographs of plunge jet into water
- Figure 6 Schematic of MIXA test setup
- Figure 7 MIXA experiments: melt front locations and water level swell
- Figure 8 Schematic of PREMIX test facility
- Figure 9 Diagram of ALPHA Test facility
- Figure 10 Conceptual Diagram of ALPHA-MJB test equipment
- Figure 11 FARO experimental facility
- Figure 12 Schematic of SIGMA-2000 test equipment
- Figure 13 IKE-multijets test facility
- Figure 14 KROTOS test section and pressure vessel
- Figure 15 Flow regime map used in PM-ALPHA code
- Figure 16 Flow regime map in JASMINE code

1. INTRODUCTION

Direct contact between hot liquid (e.g. molten metal) and volatile cold liquid (or coolant) may result in an energetic vapor explosion [sometimes called an energetic fuel-coolant interaction (FCI)]. The explosion is due to rapid heat transfer from the hot liquid to the volatile cold liquid; thus the coolant vaporizes at high pressures and expands and does work on its surroundings.

A conventional vapor explosion is generally considered to involve a progression through the stages of coarse mixing (or premixing), triggering, propagation, and expansion. In the premixing phase, generally the hot liquid is broken down into smaller sizes due to fragmentation process (coarse fragmentation). A vapor film is created at the interface of the two liquids as the cold liquid vaporizes since the first contact. The system could remain in this non-explosive metastable state for a delayed period. Triggering is the event that initiates the very rapid increase of local heat transfer and vapor pressure due to vapor film destabilization followed by fine fragmentation of the hot liquid. This "explosive" vapor formation spatially propagates throughout the mixture and thus causes the macroscopic region to become pressurized by the coolant vapor. Subsequently the high-pressure vapor coolant expands against the surroundings.

In postulated severe accidents in current fission reactors, vapor explosions are considered if this molten fuel contacts residual water in-vessel or ex-vessel because the mechanical work produced during explosion has the potential to contribute to reactor vessel failure and/or containment failure. Accidental vapor explosion have occurred also in the metal-casting industry^{1,2}, liquefied natural gas (LNG) spilling over water during transportation³, and lava flow into sea water^{4,5}. The influence of vapor explosions in nuclear reactor safety and the available studies of vapor explosion have been reviewed by, among others, Cronenberg⁶, Corradini et al.⁷, Corradini⁸, Fletcher⁹, Moriyama et al.¹⁰, and Park et al.¹¹

In the past, most work was performed to address the α -mode failure issue, a postulated event in which an in-vessel steam explosion causes the reactor vessel to fail and generates a missile that causes the containment to fail, which leads to a release of fission products to the environment. Thermodynamic approach of vapor explosion by Hicks and Menzies¹² results in an ideal thermodynamic conversion ratio of about 30%. Considering this conversion ratio and the quantity of the core debris might be resulted from a severe accident (e.g. TMI-2 accident), the integrity of reactor containment might be threatened. Since

then, numbers of research works had been performed.

The thermodynamic approach had been performed in order to predict the mechanical work produced from a FCI without taking into account the mechanisms of interaction (e.g. work done by Hicks and Menzies¹², and also Hall¹³). The results of such approach predicted generally a high value of mechanical energy liberated to the environment. To be more realistic, the approach considering the mechanism of interaction must be taken into account. Then, the experimental and analytical works had been conducted in many laboratories. Most of the early studies emphasized to examine the molten fuel fragmentation mechanism by using single drop of molten metal (see for example Nelson et al.¹⁴). During the time, the studies were developed.

Following the progress made in vapor explosion researches during more than a decade, it is generally accepted that the likelihood of α -mode failure is very low¹⁵. The combination of events leading to α -mode failure would be very unlikely. However, an improvement in the understanding of vapor explosion mechanisms is still required especially in reactor geometry and with the prototypic materials.

The premixing phase has been researched extensively in the past. However, the additional researches either experimental or analytical are still needed in order to fully understand the phenomena, especially the physics of melt jet fragmentation and subsequent coarse mixing as the molten fuel comes in contact with water. The understanding of the phenomena is important to provide a basis for estimating the spatial distribution of melt, vapor (steam), and water at the instant a trigger is postulated to initiate a propagating interaction¹⁶.

Triggering could be caused by an instability at the melt-coolant interface and subsequent collapse of a vapor film locally around a melt drop. Recent studies are emphasized to answer some topics in the triggering area, such as pressure effect on triggering, and triggerability of prototypic melts.

In point of view for resolving the α -mode, a knowledge of propagation phase details is not necessary. But, other FCI issues such as shock loading of structures, lower head loading, etc. would require such details. The 1D propagation models and codes are believed adequate at this stage. However, multi-dimensions models and codes must be developed further.

This review is aimed to collect information of recent experimental or analytical (codes development) works in premixing and propagation stages. Such kind of information is very important to know the latest status of activities and to plan the future works.

2. EXPERIMENTAL WORKS

2.1 PREMIXING STUDIES

The mixing stage (or called as premixing), during which the hot, molten material forms a coarse mixture with the coolant, is an important issue. This is because the nature of this mixture probably determines both the efficiency of conversion of thermal to mechanical energy during the subsequent stages, and the mass of material involved in the interaction. On the other hand, the degree of quenching of molten material as it falls into the coolant (or the lower plenum) is also important point. This will determine the nature of the debris resting on the bottom of the vessel (or lower head) and therefore will have a strong influence on the timing of lower head failure.

Past researches on fuel-coolant mixing has been mainly emphasized on predicting the physical limits at which mixing could or could not occur^{17,18}. The first series of experiments to understand fuel-coolant mixing progression had been conducted in Sandia National Laboratories (SNL)¹⁹, and also at Argonne National Laboratory (ANL). On the basis of need to better understand the fundamental mechanisms and the need to improve of computational methodologies in this aspect, several experiments has recently been conducted. The most important experimental works are resumed in the followings.

2.1.1 MAGICO Experiment

MAGICO experimental facility was set up at University California of Santa Barbara (UCSB), USA. The experimental study addresses certain fundamental aspects of the premixing phase during fuel – coolant interactions. The experimental results provide data for the validation of PM-ALPHA code. The experiments consist of pouring metal particles (balls) into the water pool. The first test series were done using tens-of-kilograms quantities of mm-size steel balls heated up to 1000°C^{20,21}. The key measurement in these experiments was the space-time evolution of the liquid fractions, in the two-dimensional evolving mixing zone, during the short transient. For that, a new instrument, so-called FLUTE, had been invented. This instrument could provide the instantaneous readings of the local liquid fraction.

The second test series involved various particulate materials heated up to

2000°C, hence the name, MAGICO-2000²². The schematic of MAGICO-2000 experimental facility is shown in figure 1.

Two run series were conducted, namely cold run and hot run series. The table 1 and 2 show the specification of these run series.

From cold run series, the radiographs show the formation of a "hole-in-the-water" behind the cloud and the dense packing of particles produced at the front. Since the later solid particles fall within the gas hole, they still accelerate and meet the particles front at higher velocity, push downward and sideways. This "hole" closed up a shorter time later. Using steel, the front of cloud particles reaches the bottom faster. One could also observe the presence of instability at the penetrating front. Figure 2 shows the contour lines of one experiment. In this cold run series, the volume fraction of solids in the cloud before entering the water is estimated about 10-14%.

In terms of the penetration behavior and instabilities, the results from the hot runs were found to be quite similar to those observed in the cold runs.

The combination of low particle density (using SiC) and zero subcooling condition cause the particles to undergo a strong deceleration. The higher coolant subcooling condition produced an insignificant void.

More recently, a series of test runs have been conducted in MAGICO-2000 with 2D slab geometry (100 cm length, 20 cm width)²³. The experiments is directed to produce much diluted cloud of particles (low particles volume fraction), i.e. 0.5% with pour length 6.5 m and pour duration 1.5 s. A total of eight experimental (2 runs on cold condition and 6 runs on hot condition) were investigated. All of the runs use ZrO₂ particles. Table 3 and 4 give the conditions of the runs.

The radiographic images from the cold runs show clearly the formation of the "hole" behind the cloud, and its closing the short time after (~0.35 s). These results confirmed the previous tests.

In the hot runs, the small particles (2 mm) produced highly voided regions (90% to 100%) even under 10°C subcooling, although in later case voided region was limited in size. With large particle (7 mm), one could be shown the difference in premixing regime between dense cloud and dilute cloud. In the dense cloud, the dense packing of particles produced at the front. Contrarily, in the dilute cloud, the particles are distributed almost uniform along the jet. With the same particle temperature, the void fractions are evaluated in the range of 90 to 100% and 60 to 70% for dense cloud and dilute cloud respectively. In the three dilute runs, the

particle volume fractions in the mixing zone were found to be in the 0.6 to 1.1 % range. The change of particle's temperature from 1650°C to 2000°C does not appear to have a significant effect on the resulting premixture. However, the further explanation of what the authors call "the inertial regime" (in case of dense cloud) and "thermal regime" (in case of dilute cloud) of premixing is not given yet.

2.1.2 QUEOS Experiment

QUEOS facility is set up at Forschungszentrum Karlsruhe (FZK) of Germany to study the premixing phase in fuel – coolant interactions. As in MAGICO experiments, in the QUEOS experiments, the melt is simulated by large numbers of small solid spheres in order to obtain data for code validation under well defined conditions²⁴. The materials used are ZrO_2 and Mo. With mass ranging from 7 to 20 kg, this lead to sphere numbers between 2300 and 49000. The spheres were released as a cylindrical jet into a three-dimensional test vessel containing water. The vessel is closed and connected to the atmosphere through a venting pipe (see figure 3). The test vessel is made of stainless steel frames and glass and has a square cross section of 0.7 m side length and 1.38 m height. The vent pipe is located at upper end of the test vessel. The water was uniformly heated except for a cool layer at the bottom of the tank (~0.1 m height).

The hot test runs and the cold test runs were conducted. The initial conditions of the hot tests are given in table 5. The volume fraction of the particles in the cold runs was about 53%, and approximately 25% in hot runs.

From cold runs, one could be observed the formation of gas channel behind the cloud of spheres. The first spheres touched the water with a velocity of 5 m/s, and are decelerated to about 3 m/s. The succeeding spheres pushed the first spheres sideways and downward, thereby opening a gas channel. Subsequently the diameter of this gas channel was pinched and collapsed (700 ms) trapping large bubble within the sphere cloud, which rise to the water surface at a later time.

The behavior of hot spheres is essentially similar. The generated steam flows countercurrent to the stream and leaves the water pool as a large bubble. The small spheres generate more steam than the large spheres. The pressure rise is higher. This is also the case for the large total sphere volume.

The behavior of the spheres during their fall through the water could also be seen in their relative distribution on the vessel floor. Approximately one third of all spheres was found in the center. The heavy Mo-spheres spread less than the

lighter zirconia spheres. The large zirconia spread most. Figures 4 shows the high speed photographs for one cold test .

2.1.3 BILLEAU Experiment

In order to investigate premixing phenomena, BILLEAU experiments were conducted in French Atomic Energy Commission. BILLEAU is an analytical two-dimensional experiment. Hundreds of cold or hot solid spheres stacked into tubes are poured into water. The spheres released represent a plane jet.

The experimental apparatus consists of: (1) a plexiglass water tank of 1 m long, 1 m height and 1 m width, and (2) a sphere release device. In plexiglass water tank, a test section composed of two plexiglass plates are located. These two plates defining the water slice whose thickness could be varied. In the other part, the sphere release device consists of a series of parallel tubes where the spheres were stacked. It is located at the center of the water tank. The test apparatus is completed by a high speed cine-camera.

Several tests have been conducted. The first series of test had been performed using solid sphere of DURAL ($\rho=2.7 \cdot 10^3 \text{ kg/m}^3$) and Stainless Steel ($\rho=7.8 \cdot 10^3 \text{ kg/m}^3$), at cold condition²⁵. The table 6 gives the initial conditions of the first test series. The second test series used ZrO_2 ²⁶. One test was done with glass spheres. The data obtained from the tests are: the volume fraction, the sphere velocity, the free level swell, and the final distribution of spheres. These data is useful for the validation of premixing code, i.e. MC3D code.

From FPD98 test, one could be observed that about 0.4 s after entering the water pool, the jet has taken the classical mushroom shape at its front. This is followed by an unstable column. About 0.2 s later the column disappeared; spheres are in front ball. The tests with stainless steel result a higher velocity at a same instance. The penetration of the jet is faster. We could also see the longer column of spheres.

Figure 5 shows the results of two tests using Dural and stainless steel spheres of experiment FPD98 and FPA97 respectively.

2.1.4 MIXA Experiment

MIXA experiments were conducted at AEA Winfrith Technology Center (UK)²⁷. The experiments were aimed to simulate the premixing phase during fuel-coolant interaction using prototypic materials (81% UO_2 , 19% Mo metal at a

temperature of 3600 K). The quantity of fuel used was up to 5 kg, initially in the form of droplets. The results of these experiments were used to validate the CHYMES computer code.

The experimental equipment is shown in figure 6. It consists of a charge container in which molten fuel is generated, and a mixing vessel where the mixing took place.

The initial conditions and main results of the experiments are given in table 7. The length of the skirt determines the spread of the stream as it fell to the water surface; longer the skirt, lesser the stream spreads. In all cases the water temperature was initially uniform near to saturation. The initial pressure was 0.1 MPa. The quantity of melt delivered in each experiment was approximately 3 kg. A well ordered flow of droplets was produced with diameters in the range 1 mm to 10 mm and velocity entry to the water of about 5 m/s. The pour of melt lasted for between 1 and 1.5 s.

No steam explosions were observed in any of the experiments. From the cine-film obtained, one could be observed the deceleration of the melt droplets as they entered the water. The steam generation was sufficient to arrest the hot melt droplets and suspend them in a fluidized state. This lead to accumulation of melt in the fluidized region but despite this, no re-agglomeration of melt droplets was observed.

After a while the front developed irregularities (suggested a Rayleigh – Taylor – like instability) and droplets began to fall faster. As mixing proceeded, a highly voided steam chimney formed within the mixture, and this clearly allowed steam to flow upwards, escaping from the mixture. The melt front location and water level swell are shown in figure 7.

The effects of concentration of the melt droplets were obviously observed from the experiments. In low concentration of melt droplets (MIXA01), the suspension of the melt was most pronounced, the voiding was less important.

2.1.5 PREMIX Experiment

PREMIX test facility was set up in Forschungszentrum Karlsruhe, Germany²⁸. The major goals of the tests conducted in this facility are to study the inherent limitation of the masses involved in premixing and to obtain data for verifying and validating the computer codes.

A series of experiments is being performed using a hot alumina melt discharged

into the water pool. The main parameters have been: the melt mass, the number of nozzles, the fall height, and the depth of the water.

A scheme of experimental apparatus is shown in figure 8. Principally, it consists of a cylindrical vessel with four venting pipes at upper end. Inside the upper part of the vessel, the thermite melt generator was mounted leaving an annular gap between its casing and the vessel wall. The melt release, driven by a small pressure difference (0.08 MPa), occurs through the nozzle fixed at the bottom of the melt generator. At the bottom part, the fragment catcher was located. Besides the collection particles, this catcher was used to investigate the spreading of a liquid melt arriving at a flat bottom. The vessel is filled with the water to a desired level. At the front and rear side of the vessel, glass windows were installed enabled high-speed and video filming.

Eleven test runs have been performed. The last two tests, PM10 and PM11, have been performed to investigate the influence of smaller water depth in combination with a larger mass of melt. In PM11 test, a triple nozzle was used instead of single nozzle while keeping the nozzle cross section be constant.

In PM10, the explosion did not occur. In PM11, the explosion occurs at about 1 s after the melt release destroying the facility. The authors estimated the peak pressure of about 3 MPa and the mechanical work release less than 100kJ.

2.1.6 ALPHA Experiment

In order to clarify the phenomena which could threaten the containment integrity and to evaluate accident management measures, Japan Atomic Energy Agency (JAERI) initiated in 1990 a research program called Assessment of Loads and Performance of Containment in a Hypothetical Accident (ALPHA). The objectives of ALPHA program are to evaluate the mechanical loads to containment, to characterize the leakage behavior through containment penetrations and to assess the possible accident management measures^{29,30}.

The ALPHA program consists of the molten core coolant interaction tests, the molten core concrete interaction tests, the containment leak characterization tests, and the aerosol behavior tests. Therefore the ALPHA facility was designed and constructed to perform all of these tests. Schematic diagram of ALPHA Facility is shown in figure 9. The detail of ALPHA facility design is reported by Yamano et al.³¹.

The fuel – coolant interaction experiments are one of test series of molten core – coolant interaction test, and are aimed to quantify the loads to the containment

during fuel – coolant interactions (FCIs) and to evaluate coolability of the molten core. For this series of tests, the model containment vessel of the ALPHA Facility is used. The model containment vessel has an inner diameter of 3.9 m, a height of 5.7 m and an inner volume of 50 m³. The vessel is made of carbon steel with stainless steel liner, and designed to withstand pressure of 2 MPa and temperature of 250°C. The vessel is pressurized mainly by nitrogen gas. Several viewing windows are provided for visual observation during the experiments.

In the past, two series of test runs have been performed: melt drop steam explosion experiments (denoted as STX series) in which the stimulated molten core was dropped into a pool of water, and melt coolability experiments (denoted as ACM series) where water was poured onto the simulated core melt. The experiment conditions and the results of these two tests series are reported by Yamano et al.³².

More recently, to investigate the energetics of vapor explosions in various contact geometries between coolant and molten material, ALPHA/MUSE (Multi-configuration in Steam Explosions) experimental program was initiated³³.

Considering the importance of the premixing phase in FCIs, i.e. as initial condition of subsequent events, another series of experiments has been performed in the frame of ALPHA program (called ALPHA-MJB experiments)³⁴. The experiments are aimed to study the melt jet breakup and fragmentation in which the objectives are to provide data suitable to assess / improve the existing models and develop new models if necessary. The experiments are still underway, and it is planned to perform systematic experiments to investigate the effect of various parameters such as velocity and diameter of melt jet, density, temperature, surface tension of the jet material, temperature of water and ambient pressure³⁴. In parallel with the experiments, JASMINE (JAERI Simulator for Multiphase Interactions and Explosion) code has been developed to analyze the whole process of the steam explosion.

The test apparatus used for the ALPHA-MJB series experiments is schematically given in Figure 10. It consists of melt generator in upper part and the water pool in the lower part. The water pool has a cross section of 83 cm x 83 cm and 3 m depth. It is made of steel frame and transparent polycarbonate panels. To heat up and maintain the pool water, steam was injected from the bottom of the pool. The steam generated in the water as a result of melt - coolant interaction was exhausted by a pipe with diameter of 210.7 mm. At the end of the exhaust pipe 82.5 mm diameter orifice is located. By measuring the pressure

difference between upstream and downstream of the orifice, steam flow rate could be calculated.

Above the water pool, the melt generator was located. It consists of a cylindrical crucible made of steel surrounded by heater and covered with thermal insulator. At the bottom of the crucible, a pipe was connected. Several pipes with different diameter were used to change jet diameter.

The behavior of the jet was recorded using a high-speed camera (2000 fps) and a high-speed video camera (500 fps).

A lead – bismuth alloy (Bi 55.5 w/o, Pb 44.5 w/o) was used as the jet material. The material is an eutectic alloy which has a constant temperature for solidification like a pure metal. The conditions of two experiments (MJB01 and MJB02) are given in the table 8.

One could be obtained from the experiments are penetration length of jet, steam flow rate and mass distribution of debris particles. The measured jet breakup length were 1450 mm and 870 mm for MJB01 and MJB02 respectively. Post-test examinations of the debris show the mass median diameter of 3.4 mm and 2.6 mm for MJB01 and MJB02 respectively. The observation of the two experiments could not show the clear vortex ball.

Therefore in order to give insight for clarification of the mechanism of the jet breakup and fragmentation, several experiments have been planned. Future experiments will uses higher temperature of melt, larger diameter and higher velocity of jet

2.1.7 FARO Experiment

In terms of safety aspects of FCIs, it has been found of fundamental importance to carry out tests involving large amounts of prototypical corium poured into water at reactor scale depth, in order to characterize the melt/water mixing and quenching process.

The JRC – Ispra FARO plant is used for such a purpose. The objective of the test series is to determine : (1) the melt quenching rate associated with the melt/water penetration, (2) the hydrogen production associated with the zirconium production, (3) the thermal loads on the bottom structure, and (4) characteristics of the debris structure³⁵.

FARO is a multi-purpose test facility in which severe accidents can be simulated out-of-pile under various conditions. Basically, a maximum quantity of the order of 150 kg of $\text{UO}_2 - \text{ZrO}_2$ fuel type melts (up to 3000°C) can be produced in the

FARO furnace, possibly mixed with metallic components (e.g. Zr), and delivered to a test section of interest. Figure 11 shows the experimental facility.

Two experiments, known as scoping test (denoted as L-06) and quenching test 2 (denoted L-08), were performed using relatively small quantities (18 kg and 44 kg) of melt. The experiments and the results had been reviewed by Moriyama et al.¹¹

Afterwards, two other experiments (L-11 and L-14) were realized in TERMOS vessel, involving large quantities (151 kg and 125 kg) of corium melt³⁶. The mass of the water used is also larger in these two tests, reducing the distance between the release nozzle and the water surface. The L-11 test differed from the other tests by the contain of Zr metal. No steam explosion was observed in any of these tests and no threatening thermal load on the bottom structure was measured. In the L-11 test, the jet experienced complete breakup before reaching the bottom of the vessel. The estimated thermal energy released during the melt fall in L-11 is much higher than in L-14; 1.13 MJ/kg compared to 0.79 MJ/kg. In all cases, the mean particle size of the broken up debris ranged between 3.5 to 4.8 mm.

The most recent experiments (L-19, L-20, and L-24) have been performed to study the effects of some important parameters (such as the initial pressure and the water depth), and together with the previous tests, the analysis has been done allowing to describe a conceptual picture of the premixing³⁷. According to the authors, this picture is based on the assumption that the breakup at the leading edge alone cannot account for the significant amount of breakup observed in the test. Thus it is proposed that erosion of the jet column (Kelvin-Helmholtz instabilities, boundary layer stripping etc.) is an efficient breakup process and the main source of breakup for large pours. In the other hand, leading edge breakup produced bigger particles. Table 9 resumes the experiments data.

Concerning to Hydrogen production, it was found that significant amount were produced in test using pure oxide melt. Because no direct measurement was possible in these tests, further improvement in the future test must be performed. It was recognized that further efforts must be done, especially to reduce as much as possible the differences in the melt/water entry conditions and to perform the conditions allowing verification of conceptual picture of mixing mechanism.

In the context of the benchmark FCI and melt quenching codes against the results of a well defined experiment, the FARO test L-14 was selected as

International Standard Problem (ISP) reference test case³⁸. This exercise involves 13 organizations with 9 FCI codes.

2.2 PROPAGATION STUDIES

In the presence of a trigger, a vapor explosion could spatially propagate. Experimental observations suggest that triggering is associated with the local collapse of the vapor layer around a melt droplet followed by rapid fragmentation of the melt droplet⁷.

The propagation can easily propagate in small-scale or intermediate-scale quantities of melt (~ 10 kg) as observed in the FITS³⁹ and SUW⁴⁰ experimental series. Photographic evidence shows the explosion occurs when a wave propagates through the mixture. However, the detailed physics controlling the propagation is still unclear.

The first model to explain the propagation is proposed by Board and his collaborators⁴¹. They postulated an analogy between steam explosion and chemical detonation. In such a thermal detonation, the energy transfer from hot fluid to the cold liquid is initiated by a shock front in a manner analogous to chemical detonation. They developed their initial simple model to explain the efficiency of interaction⁴². The further model developments are directed toward the fragmentation and heat transfer mechanisms during the passage of shock front. They have been reviewed in detail by Fletcher and Anderson⁴³.

In the following, some recent experimental tests, addressing to gain an insight into the propagation phenomena, are described.

2.2.1 SIGMA Experiment

SIGMA experimental program is performed at the University of California Santa Barbara (USA). Utilizing of SIGMA facilities, fragmentation kinetics of molten drops at various shock pressures were studied. Previously, SIGMA facility has been employed to study of mercury drops and tin drops (at about 1000°C) in water. Then, the facility is upgraded to allow melt drops temperature up to 2000K (hence SIGMA-2000 name)⁴⁴. The experimental program is performed to support the microinteractions concept proposed as the fundamental mechanism during steam explosion/propagation phase.

The schematic of SIGMA-2000 facility is shown in figure 12. The basic

component is the shock tube, consisting of a 1 m long driver section and a 2 m long expansion section. The design pressure is 1000 bar and with water in the expansion section it allows steady flows/pressures for up to 2.3 ms, before the reflected wave from the bottom end of the tube arrives back to the window area. The midpoint of the window is located 50 cm below the top of the expansion section. Through this window, observation by means of X-ray and high speed movies camera is performed.

The melt generator is placed about 5 cm above the window. It is designed to melt and reproducibly release single drops of melt at temperature up to 2073K.

At the bottom part, the debris catcher is placed.

Several materials are used as drop, e.g. tin, gallium, steel. The major results of tin and gallium experiments with the interpretation of ESPROSE.m code are given by Chen et al.⁴³. The tests with gallium represent an isothermal interaction. The test using steel is conducted to study the importance of thermal effects⁴⁵.

In test with steel, two shock pressures, i.e. 68 bar and 265 bar, were applied. Two of the six experiments are conducted with 6% void. The collapsing of the void by the shock wave creates a high coolant velocity at the point of fuel-coolant interaction thus allowing to obtain higher velocity for the same pressure behind the shock.

Examination of the collected debris shows significant fraction of fine debris. Authors suggest as a clear evidence of a stronger fuel-coolant interaction in two-phase runs.

2.2.2 IKE MULTI-JET Experiment

A Study of the propagation of fuel-coolant interaction has been carried out at Institut für Kernenergetik und Energiesystem (IKE), University of Stuttgart (Germany), using a so-called droplet curtain arrangement (a three-dimensional arrangement of the melt droplets) of molten tin in water^{46,47}. The droplet curtain was used to overcome the problem of reproducibility encountered in the previous experiments using a single droplet chain. The main objective of the multi-jet experiment is to study the phenomenon of propagation in cases far removed from thermal detonation conditions.

Figure 13 shows a sketch of experimental facility. The crucible (1) in which the tin is melted and heat-up to the desired temperature is fixed on a frame (2). The steel rope (3) tilts the crucible by about 90° allowing the molten tin flows through the holes (4) into the water container (5). The bridge wire explosion device (7) is

placed in one side of the water container. The explosion gives a peak pressure of 32 bar at the first jet.

The molten tin flows out of the holes of crucible in the form of jets. The distance between these holes (so-called inter-jet distance) varies from 95 to 25 mm keeping the distance between first and last holes constant at 220 mm. The diameter of the holes varies also, i.e. 2, 5 and 10 mm. In all cases, the drop chains do not fall in a straight line downwards, the jets disintegrate and the droplets drift in all directions during their fall. However, the average droplet size is governed by the hole diameters. In some experiments, copper shield plates are inserted in the water container, so that individual jets or droplet chains are separated from each other.

The results obtained with the variations of the inter-jet distance show that larger the inter-jet distance lower the probability of thermal interaction propagation. At the inter-jet distance of 95 mm, no propagation was observed. For the distance of 25 mm, an average propagation velocity of 4 m/s was evaluated. In other part, the larger size of diameter of droplet leads to more violent interaction, and higher propagation velocity. The existence of copper shield between individual jet did not suppress the propagation, although the propagation velocity diminishes.

Considering the experimental results, the author concluded that the propagation of the interactions take place in jumps from one center to others; a shock waves may trigger an interaction and this interaction center produces a new shock waves during its collapse which may also trigger further interactions. Only shock waves of sufficient strength may trigger the new interaction centers. This is contrary to that of thermal detonation model in which a shock wave passes the melt-water mixture and fragments all melt droplets during its passage.

2.2.3 KROTOS Experiment

KROTOS Facility has been setup in JRC – Ispra to support FARO Program, a fuel – coolant interaction research program in the context of severe accident in nuclear power plants. Specifically, KROTOS facility is used to support the large scale tests FARO. Several tests have been performed with various simulant material, such as tin and alumina, Al_2O_3 , or with prototypical corium mixture (80 w% UO_2 + 20 w% ZrO_2). The objective of the tests is to provide data basis to investigate premixing in subcooled and saturated water, and to study the energetics of triggered or spontaneous explosions.

The experimental setup, procedure and results of the first test series (narrow test

section) in aluminum oxide/water system (KROTOS 26 – 30, and 38) and corium/water system (KROTOS 32, 33, 35, 36, 37) were reported^{48,49}, and had been reviewed by Park et al.¹¹. These experiments had been performed in small diameter of test tube, e.g. 95 mm, except for KROTOS-37 and 38 were performed in larger test tube, e.g. 200 mm.

From this test series, one could retain the difference between the tests KROTOS-30 and 38 (for Al_2O_3 /water) and KROTOS-33 and 37 (for corium/water) which were conducted in same initial conditions that energetic explosions were generated with Al_2O_3 but not with corium mixture⁴⁹.

Recently, a test series using Al_2O_3 and Corium in the large test tube have been conducted⁵⁰. The main focus of the recent KROTOS experiments is to examine the differences in mixing behavior and "explosivity" between alumina and corium melts.

Figure 14 shows KROTOS large test section and pressure vessel. The description of the KROTOS test arrangement and test procedures could be found in the previous papers.

The initial conditions of the recent test series using Al_2O_3 is given in table 10. As in the previous test series, alumina melt poured in subcooled water (~ 80 K) at ambient pressure generated, independently to melt superheat, spontaneous critical explosions with propagation speeds in excess of 1000 m/s. During the pre-mixing phase the average integral void fraction varied from 1.0% to 2.6%.

In the other hand, with near-saturated water pools, the external trigger pulse must be given to generate the explosions. The void fractions in these tests were higher, and varied from 10% to 30%.

Augmentation of ambient pressure to 0.2 MPa and 0.375 MPa in highly subcooled water pools, did not suppressed the spontaneous explosions. The integral void fractions are about 1.9% and 0.6% during the pre-mixing phase.

With corium/water system, four tests have been performed in the recent test series (KROTOS 37, 45, 47 and 52). The initial conditions and main test results are presented in table 11. No steam explosions have been obtained with highly subcooled or near-saturated water pools. High integral void fractions, i.e. 13% to about 30%, were measured during pre-mixing phase. It was also observed that the pressurization in the pressure vessel remained high in the long term indicating generation of non-condensable gas, i.e. hydrogen, during the corium/water interactions. Elevated pressure reduced the integral void fraction. By comparing the results between alumina and corium melts, Huhtiniemi et al.⁵⁰

show and interpret the differences in melt penetration, pour breakup and fragmentation behavior as the follows. Alumina melt pours decelerates faster than corium pours at the water surface due to lower density. It is likely that the deceleration also enhances early breakup of the melt pour and its lateral spreading. It would also suggest that alumina melt most likely existed as larger diameter melt globules which implies smaller surface to volume ratio thus reducing the steam generation and further breakup. These conditions might form a suitable coarse mixture for an energetic explosion to take place if a trigger is provided. On the contrary, the corium melt pour is observed to penetrate deeper as a coherent pour. So, the authors suggest that fine fragmentation at leading edge of the melt pour takes place and resulting steaming paves the way for the coherent core to penetrate.

3. CODES/MODEL DEVELOPMENTS

While the experimental studies on fuel-coolant interactions are being performed, the need for a thermal-hydraulic code that could analyze so complicated phenomena is identified. The existence of such code is also needed to be a scaling tool bridging the experimental findings and the real scale geometry.

In the followings, the important existing codes for fuel-coolant interaction analysis, especially the premixing phase and the propagation phase, are described. The intend is to highlight the major features of the codes (e.g. the jet fragmentation, the melt drops breakup, and certain constitutive laws). The detailed description of each code and the verification results can be found in the references.

3.1 IFCI Code

The Integrated Fuel-Coolant Interaction Code (IFCI), developed at Sandia National Laboratories (USA), is a best-estimate computer program for analysis of phenomena related to mixing of molten nuclear reactor core material with reactor coolant (water)⁵¹. The code is intended to address all aspects of FCI phenomena, including coarse fragmentation and mixing of molten material with water (premixing), triggering, propagation and fine fragmentation, and expansion of the melt-water system. The stand-alone version, IFCI 6.0, of the code has been designed for analysis of small and intermediate-scale experiments in order to gain an insight into the physics of molten fuel-coolant interactions.

IFCI is developed based on MELPROG/MOD1 using of SETS (Stability-

Enhancing Two-Step) hydrodynamic method. This method satisfied the multifield and compressible hydrodynamic criteria.

The equation set used in IFCI is a four-field, two-dimensional, cylindrical geometry (r-z geometry). The four fields consist of vapor (steam), water, solid fuel, and melt. But, actually the solid fuel field is not applied yet. A field means a set of momentum, mass continuity, and energy equations; a separate set of these equations is solved for each field. The equations are formulated on Eulerian field. Mass, energy, and momentum transfer between fields is represented by coupling terms in these equation sets.

Constitutive relations are provided in IFCI for heat and momentum transfer in the bubbly, slug, and mist flow regimes between water and vapor. Flow regimes for the melt field are derived by treating the water and vapor together as a second phase. The melt is then described on the melt volume fraction, as either continuous with entrained vapor-water droplets, or as melt droplets in a continuous vapor-water phase.

The fuel characteristic size may either be smaller than a mesh cell (i.e. sub-grid size) or extend over more than one cell. In the sub-grid case, the fuel melt exists as discrete drops. IFCI treats with the fragmentation model. In the case the melt extent is larger than the mesh cell size, surface area generation takes place as the melt geometry distorts due to hydrodynamic motion on the grid. IFCI uses a surface area tracking model. The melt fragmentation model in IFCI is a version of a dynamic fragmentation model developed by Pilch based on Rayleigh-Taylor instability theory and the existing body of gas-liquid and liquid-liquid drop breakup data. The surface tracking algorithm is based on Volume-Of-Fluid (VOF) method. The film boiling regime, which is dominant regime during interaction, is described from sub-cooled boiling correlations of Dihr and Purohit. Comparison of code with the experimental data has been performed. Satisfactory validation results against non-exploding FITS-D series experiments had been reported⁵². IFCI is also used by several organizations in OECD/CSNI ISP-39 on FARO Test L-14.

3.2. TEXAS Code

TEXAS computer code is a major tools used at the University of Wisconsin for simulations of fuel-coolant interaction during its mixing, triggering and explosion phases. TEXAS is a mechanistic model used for FCI analysis⁵³. The original TEXAS code was a parametric model developed by Young⁵⁴ for the design and

analysis of fuel-coolant interaction experiments for LMFBR safety related issue. In order to extend the capabilities of TEXAS, especially in terms of fuel-coolant mixing, Chu and Corradini⁵⁵ incorporated a dynamic fragmentation model and a complete set of constitutive correlations for interfacial mass, momentum, and energy exchange terms; i.e. TEXAS-II. The improvements of TEXAS had been performed to include the explosion propagation, i.e. TEXAS-III⁵⁶.

The model solves the one-dimensional, three field equations describing the fuel, coolant vapor and liquid. Two fields represent the coolant as separate liquid and vapor in an Eulerian control volume, while one-field models the fuel as discrete material volume in a Lagrangian formulation.

Originally, the hydrodynamic fragmentation of the fuel based on Rayleigh-Taylor instabilities (RTI) is considered during mixing phase. Deceleration forces as well as deformation of the jet or drops determine the driving forces for the instabilities, which can lead to breakup the jet leading edge or falling drops. As an approximation, the molten jet is taken to be composed of a series of discrete particles that enter the coolant sequentially with the jet leading edge by the relative position of the first unfragmented master particle compared to the position of the master particles preceding it. A multistage breakup process with breakup in discrete steps results until the diameter is small enough that the instantaneous Weber number falls below the critical value. The drops break up during mixing is formulated by a simplified linear correlation.

During the propagation phase, the thermal fragmentation of fuel is considered based on the model proposed by Kim and Corradini, in which the fragmentation of droplet is assumed due to evaporation of entrapped micro-coolant jet. The simplification had been made from original model due to the complexity.

Recently, TEXAS code has been improved by further insights in fuel-coolant interaction processes. The improvements deal with the hydrodynamic fuel breakup, i.e. the fuel jet entry conditions and complete jet breakup model⁵⁷. As the entry conditions, user can specify variable inflow boundary conditions for the incoming fuel jet, such as the jet radius, velocity and temperature, also the specification of how much of the fuel first enters the water pool as discrete fuel masses and then as coherent jet.

Concerning the jet breakup model, three hydrodynamic-related mechanisms are now considered during the mixing phase. Only one is considered to be dominant at any one specific location of the jet surface. The effects of Boundary Layer Stripping primarily occur at the jet leading edge. The effects of Kelvin-Helmholtz

instability are considered to be dominant at upstream of the leading edge along with the body of the jet. Finally, the RTI mechanism dominates the breakup the discrete particles separated from the jet.

FARO L-14 test run is chosen to demonstrate the TEXAS model improvements⁵⁷. In terms of integral pressure history, the new model predicts better than the original model. It is also true for the kinematics of the jet entry and arrival at the chamber base. The lack of agreement, less than 10%, is found in the prediction of the liquid temperature near the pool bottom and vapor temperature. Other deficiency of the model is its one-dimensional formulation and improvements that need to be made in the subcooled film boiling heat transfer by taking into account radiative transport model.

3.3 CHYMES Code

CHYMES code is developed at AEA Culham Laboratory (UK). The code intends to study the premixing phase of fuel-coolant interactions⁵⁸.

The model is transient, two-dimensional, either in Cartesian coordinates or cylindrical coordinates. A three component flow is modeled, consisting of a hot melt, a cold liquid (usually water) and the vapor phase of the cold liquid (i.e. usually steam). The water and steam are both assumed to be at saturation temperature corresponding to the specified ambient pressure. But, the extension of the model into subcooled condition has been considered. Viscous and turbulent diffusion processes are not included in the present model. The hot melt is assumed to be composed of spherical droplets. The hydrodynamics are modeled using the usual multiphase flow equations in Eulerian formulation. The equations are solved to determine a characteristic lengthscale for the melt and the water phase. The transport equations for interfacial area per unit mass are provided.

Heat transfer model is based on radiation heat transfer, using usual radiation heat transfer correlation, and film boiling heat transfer. The film boiling heat transfer coefficient is taken to the maximum of the forced and free convection film boiling coefficients, which are given by Witte and Dühr and Purhoit correlation respectively.

The interfacial drags are modeled by two different laws; i.e. a simple dispersed flow drag law, and a drag law based on flow regime map as used in PM-ALPHA code.

The droplet melt fragmentation is taken of model used in IFCI code RTI based

law).

The CHYMES code has been tested against several experimental results. One of the comparisons is performed with MIXA experiment⁵⁹. The code does not predict a sufficiently rapid deceleration at the beginning, but makes a reasonably good calculation at near steady condition. The final size debris predicted by the code is consistent with the experimental results.

3.4 PM-ALPHA Code

The PM-ALPHA code is developed at University of California Santa Barbara (USA). The code is specifically directed to analyze premixing stage⁶⁰. The melt is considered to enter the coolant in a broken-up configuration (droplets) of some characteristic dimension and specified volume fraction. Progressive breakup is given by a parametrical law..

There are three separate phases considered; coolant liquid, coolant vapor, and melt drops. Each phase is represented by one velocity field. The fields are allowed to exchange energy and momentum with each other, but only the steam and water fields are allowed to exchange mass. The diffusive transport within each field (shear stress and conduction) has been ignored.

The interfacial exchange laws are flow regime dependent. An approach had been pursued by defining a flow regime map. Regarding the melt volume fraction, the flow is over immersed fuel particle when melt volume fraction is smaller than 0.3, and is through a porous bed of fuel particles when the melt volume fraction is equal or greater than 0.3. In the case of flow over immersed fuel particles, the flow could be bubbly flow, churn-turbulent flow or droplet flow depending on void fraction. The drag forces are then deduced from the existing two-phase flow correlation. Figure 15 shows the flow regime map considered in this model.

The heat exchange mechanisms between phases are mainly by film boiling (Witte correlation), convection and radiation.

The system equations are solved using finite-difference scheme. The calculation could be done for two-dimensional, axisymmetric problems.

The PM-ALPHA code has been tested against MAGICO experiments^{21,22,23,61}, QUEOS experiments, MIXA experiments, and FARO experiments⁶².

3.5 MC3D Code

MC3D Codes is developed in French Atomic Energy Commission (CEA, France). Eulerian MC3D program calculates different types of multiphase,

multicomponent flow. In MC3D, specific type of multiphase flow calculation is called "an application". Each application relates to the general flow applications, i.e. fuel – coolant interactions, superheated liquid propane release, fast reactor fuel assembly and the fragmentation of liquid jet in gas.

In terms of fuel – coolant interactions, more specific applications could be designated, such as premixing, three-phase system, steam explosion (propagation), and steam explosion in a stratified geometry. Several modules were written to model these particular cases.

The three-phase system application considers three components, i.e. liquid (coolant), vapor and droplets (fuel). The premixing application models jet fragmentation by using 4-fields system, i.e. liquid, vapor (and non-condensable gas), melt jet, and melt droplets. The explosion application considers four components, four fields, i.e. liquid, vapor, droplets, and debris. The stratified geometry application considers three components (three fields): i.e. liquid, vapor and droplets.

The early version of three-phase application was validated with FARO scoping test (ST) and quenching test (QT2)⁶³. Since, the improvement of the code was performed. The improvement is performed to take into account: solidification of the droplets, and the process of primary break up (associated to the source term in interfacial area transport equation). The improved code is validated against BILLEAU experiments and FARO L-14 test⁶⁴.

The premixing calculation module of MC3D is an extension of three-phase module. Here, the melt is described in 2 fields: jet and droplets issued from the jet fragmentation. A detailed fragmentation model is not implemented here. But, based on the study on steam film temperature and velocity profile, and instability development, several parameters of jet fragmentation model could be estimated⁶⁵. These parameters are: fragmentation rate (thin and thick vapor film), droplet size. The jet boundary tracking is based on the Volume-Of-Fluid (VOF) method. The breakup of the jet occurs in this boundary and is proportional to its area. The droplets leave the jet with the same velocity of the jet. The jet ceases to breakup if the velocity is lower than lower limit value. The corium jet transfers energy to water only by radiation. The droplets breakup model is same as in three-phase application. The source term corresponds to droplets stripped from the jet and from fragmentation of droplets. The premixing application of MC3D had been tested against FARO L-14 test.

The explosion module of MC3D code is developed to model the fine

fragmentation phase and the explosion⁶⁶. The model consists of four fluids (i.e. liquid coolant, vapor, fuel drop and fuel fragment) and four velocity fields. During the calculation, the pressure could be sub-critical or supercritical. To do so, the equation of state of water is extended to the pressure of about 100 MPa. The flow configuration determining the exchange laws depends on the void fraction. In all cases, the fuel drops and fragments are always as dispersed phase. Two mechanisms of fuel drops fragmentation are considered, i.e. thermal fragmentation and hydrodynamic fragmentation. The thermal fragmentation rate, due to destabilization of vapor film, is given as cosine fragmentation law. The time of fragmentation, the mass fragmented and the diameter of fragments are parametric. The hydrodynamic fragmentation rate, due to velocity difference of drops and continuous fluid. The heat transfer model in general is similar to one of premixing module of MC3D. The heat transfer between fragments and interface of liquid coolant, which is highly transient, is approximated by constant value of the order 10^5 W/m²/K. Comparison with KROTOS-21 test had been done.

3.6 JASMINE Code

JASMINE (JAERI Simulator for Multi-phase Interaction and Explosion) has been developed at JAERI establishment (Japan). The final scope of the code is to analyze whole process of the steam explosion, and to serve as a scaling tool to bridge the phenomenological models developed from experimental findings and the real scale of reactor condition. At current time, the development of JASMINE code is directed to build two calculation modules, i.e. premixing module (-pre) and propagation module (-pro)⁶⁷. The development of JASMINE is supported by ALPHA experiments program.

JASMINE-pre is a 3-dimension, multi-phase and multi-fields simulation code based on finite difference method^{68,69}. JASMINE premixing module solves the mass, momentum and energy conservation laws for water, steam and melt fields using Eulerian description. The melt consists of continuous jet and droplets. The constitutive equations of the melt are averaged using jet fraction in the melt field. In the current model, the continuous melt jet must be in the center node.

A one-dimensional mass conservation of the jet column is introduced. Originally, the melt jet break up model is based on the Rayleigh-Taylor instability. Then, the Kelvin-Helmholtz instability derived from Epstein and Fauske is added. The source term of the melt surface is expressed by a simplified law. This law

contains a parametrical constant, which must be tuned against experimental data. The melt droplet break up model is similar to the one described in IFCI code. The exchange model is derived considering a flow regime model. Figure 16 shows the flow regime map.

The model has been tested against several experimental results: e.g. the isothermal mixing experiment of solid particles (Gilbertson et al.) and hot particle-water mixing of MAGICO experiment⁶⁹, FARO L-14^{68,70}, and ALPHA-MJB experiment³⁴.

3.7 VESUVIUS Code

In order to analyze the ex-vessel steam explosion events, Nuclear Power Engineering Corporation (NUPEC) of Japan develops VESUVIUS (Vapor Explosion Simulation Under Ex-Vessel Conditions for the IMPACT NUPEC Software) Module. VESUVIUS module is being developed as a stand-alone module which will ultimately be incorporated into NUPEC's IMPACT simulation software⁷⁰. VESUVIUS aims to predict all phases of the vapor explosion process. VESUVIUS is multi-dimensions, multi-fields thermal-hydraulics computer code. Four phases are considered here, i.e. liquid coolant, vapor, molten fuel jet and fuel droplets. The droplets break up model is adopted from IFCI model (i.e. Pilch correlation). The constitutive laws are based on flow regime map similar to PM-ALPHA code. Comparison to the MIXA test and PM-ALPHA code had been done⁷¹.

In order to take into account the flow of continuous phase of molten debris, the jet break up is modeled^{72,73}. The jet breakup due to surface stripping, specifically Kelvin-Helmholtz instabilities. The leading edge break up is not modeled. The jet, which is surrounded by vapor film, is modeled as one-dimensional and axisymmetric. The jet is limited to being in the center radial cell. The Mass and momentum conservation equations for the vapor film surrounding the jet are solved separately to obtain the film velocity and thickness. These last are important to the calculation of Kelvin-Helmholtz instability.

The verification calculations of VESUVIUS jet break up model have been performed against FARO L-06 test run⁷³.

3.8 THIRMAL-1 Code

THIRMAL-1, developed at Argonne National Laboratory (USA), calculates the non-explosive fragmentation and quenching of a melt stream inside a water pool

as well as the associated water heatup, net steam formation, oxidation, and hydrogen generation⁷⁴. THIRMAL-1 is the improved version of THIRMAL-0⁷⁵.

THIRMAL-1 treats the case of a circular melt stream entering the water pool with a time varying diameter, velocity, temperature, and composition. THIRMAL-1 models the breakup of a coherent melt stream due to the growth of wave instabilities along the stream surface. The dominant fragmentation mechanism is the erosion of molten droplets from the surface of the melt stream due to the formation of Kelvin-Helmholtz instabilities. The droplet diameter is assumed to be equal to the inverse wave number of the local fastest growing wavelength, and is determined at the instant of erosion from the melt stream. In particular, once the droplet is created, no further breakup of the droplet into smaller sized fragments is modeled.

A mixing zone containing the melt droplets and two-phase water surrounds the melt jet. Depending on the local condition, the flow in the mixing zone might be bubbly flow, churn flow or dispersed flow.

In current version, THIRMAL-1 accounts for the presence of distinct oxide and metal phases in the melt entering the water. In particular, individual droplets eroded from the melt stream are modeled as consisting wholly of either oxide or metal. This approach permits oxide and metal droplets to freeze at different temperatures.

THIRMAL-1 also models oxidation of the metallic droplets and particles as they relocate through interaction zone (the multiphase zone contains melt droplets, melt particles, water, and steam) and water pool

The calculation in THIRMAL-1 is performed in one dimension with Eulerian treatment for the coolant liquid and vapor, and Lagrangian treatment for the melt. THIRMAL-1 has been used to analyze the melt breakup, quenching, and debris formation inside the water flooded lower drywell region of the Forsmak 3 BWR following an hypothetical failure of the reactor vessel lower head⁷⁶. Comparison of THIRMAL-1 with FARO experiments (scoping test and quenching test), and also CCM experiments (at Argonne) has been performed⁷⁷.

3.9 IKEJET Code

IKEJET is a melt jet breakup model developed at Institut für Kernenergetik und Energiesysteme (IKE), University of Stuttgart (Germany). This code is to describe the melt jet breakup processes as condition for premixing. The model of jet breakup is essentially based on the stripping of fragments from wave

produced at the surface of the jet column due to the relative flow of the surrounding medium^{78,79}. The model is applied mainly to non-boiling and thick film boiling conditions

The description of the model consists of the jet dynamics, the vapor film boiling, the wave growth and stripping at the jet columns. The transient jet behaviors are given in one-dimensional approach. A vortex ball at leading edge is not considered. The vapor film boiling has been modeled in a quasi-steady approach neglecting entrainment of water droplets in the film and of vapor bubbles in the liquid. Model of wave growth considers the Jeffry-Miles formulation, assuming a logarithmic profile of flow in turbulence vapor shear layer. As a comparison, the Kelvin-Helmholtz jump formulation is considered. A direct stripping of crests of waves, having grown beyond half of the wavelength, is considered.

Parametrical calculations had been done to check the model against the experimental results. The experiments considered are those of non-boiling and film boiling jet experiments, such as: Wood's metal/water experiments at IKE, ANL, and JRC-Ispra, corium/water experiments at ANL and JRC-Ispra.

In an attempt to elaborate the model, a multiphase approach for vapor region is considered to take into account the possible influence of the fragments and water droplets in the vapor film region⁸⁰. A formulation has been chosen setting the locally produced finely fragmented part, assumed to be carried instantaneously by the flow, proportional to the local stripping rate. The local mean density is then calculated from the continuity equations assuming homogeneous flow.

The calculations for experiments PREMIX02 and FARO L-14 and L-20 have been done. The discrepancies of fragmentation rate and fragments size are observed. Authors explain that smaller fragment size obtained from calculation requires coalescence of fragments rather than further break up. On the other hand, the multiphase approach must be developed with emphasis on description of flow carrying fine fragments, evaporation, and heat up of vapor.

3.10 COMETA Code

The COMETA (**C**Ore **M**EIt **T**hermal-hydraulic **A**nalysis) code, developed at JRC-Ispra (Italy/EU), is a coupled thermal-hydraulic and fuel fragmentation code conceived for the simulation of fuel-coolant interaction and quenching^{81,82}. It has been specifically developed to provide a computational tool for test design and

specification, definition procedures and test result analysis.

COMETA is composed of a two-phase flow field, which is described by $6+n$ equations (mass, momentum and energy for each phase and n mass conservation equations for n non-condensable gases), and corium field with 3 phases: the jet, the droplets and the debris. The two-phase field is described in Eulerian while the corium field in Lagrangian coordinates. One-dimensional and two-dimensional nodalization could be used.

The fuel, which is modeled in three phases, is released in the form of a coherent jet. This jet is conical shaped, based on the initial discharge diameter, with a wavy and rough surface. Three models for jet fragmentation and fragment creation are included:

- the original COMETA model, based on the jet breakup length concept (The correlation from Saito, Epstein-Fauske, and mixed correlation)
- the Corradini and Tang model (similar to the model present in TEXAS)
- the IKEJET model

The drops, leaving from the jet surface during its descent, are created with an initial diameter to satisfy the Weber number criterion. Up to 500 groups of drops can be followed; each group is characterized by diameter, mass, temperature, velocity, and position providing good basis for the analysis of the statistical distribution of the debris particles. The residual part of the jet, which reaches the bottom, relocates as a cake (so-called fused-debris bed).

A model to describe hydrogen generation during the interaction phase is included in the current version of the code; a first simple model, and a second SCDAP/RELAP5 model. In addition, valves, separators, pumps, accumulators and others thermal-hydraulic components can be defined in order to fully represent the FARO test facility.

COMETA is routinely used for pre and post-test analysis of the FARO. The comparison results with FARO experiments are reported⁸¹. Calculations with FARO L-20 show that a satisfactory results are obtained with hydrogen generation model, either simple or SCDAP model, and with two-dimensional nodalization.

3.11 TRACER-II

A computer program TRACER-II (**TR**Ansient **C**omputation of **E**xplosive **R**eactions) has been developed at Korea Maritime University (South Korea) for analysis of potential impacts from a vapor explosion. The computer program

contains a complete description of mixing and propagation phases of vapor explosion⁸³.

It is postulated in the model that the melt stream breaks up into droplet when pouring into the coolant. The fuel droplets are dispersed and the vapor film exists between the hot melt and the coolant liquid. When triggering is applied, a shock wave propagates through the pre-mixture and the droplets are fragmented into fine debris. Then, rapid heat transfer from debris to coolant occurs. In the present model, a high pressure or high fragmentation rate in a cell prescribes a triggering.

The model includes four phases; fuel melt, liquid and vapor coolant, and fragmented fuel debris. The fragmented fuel debris are assumed to become thermal and mechanical equilibrium with liquid continuum upon fragmentation. So, the combination of coolant liquid (or vapor) and fuel debris are treated as one velocity field. The surface area of melt droplets is formulated using an interfacial area transport equation.

The fuel breakup rate and fragmentation are developed based on the model proposed by Fletcher^{58,91}.

The interfacial exchange laws, which is based on the local flow regimes, proposed by Angelini et al.²².

The set of governing equations are described in two-dimensional Eulerian coordinates, and solved numerically using finite difference method.

To assess the performance of the model's prediction of mixing and propagation, FARO L-14 and KROTOS-28 experiments were chosen for comparison. The comparison of mixing calculations with FARO L-14 shows a strong dependency on the empirical constant of break up model. On the other hand, the present model fail to predict KROTOS-28 experiment adequately.

3.12 IVA Code

The IVA code, developed at Forschungszentrum Karlsruhe (called IVA-KA)⁸⁴ and at KWU Siemens (called IVA4)^{85,86}, models transient multiphase flows consisting of water, steam, non-condensable gases, microscopic and macroscopic solid particles and/or molten materials. The code is developed from previous IVA-3 code. The code could consider various flow regimes. The melt jet is not modeled explicitly in the code.

The IVA-KA is multi-fluid code aiming to describe the premixing phase. The used for the propagation and expansion phase is previewed. The improvement of the

code is being performed. The QUEOS experiments is used as a data base for development of the constitutive laws. The drag laws of three-phase fluid and the radiative heat transfer are among others⁸⁷.

Three velocity fields are considered to describe the individual motion of gas (steam and/or air), liquid water and melt (hot or solid materials). The model can be up to three-dimensional, either rectangular or cylindrical coordinates.

In the IVA4, the concept of dynamic fragmentation and coalescence of all of the velocity fields is used⁸⁸. The jet fragmentation develops as function of the jet breakup length (L/D criteria). The drops are created with the diameter to satisfy the Weber number criterion. The fragmentation of the dispersed drops is governed by the Weber number criterion. The code is tested against FARO experiments⁸⁹. The calculation for analysis of in-vessel melt/water interaction for a real geometry is also attempted⁹⁰.

3.13 CULDESAC Code

The CULDESAC code is a computational model to analyze propagation stage of fuel-coolant interactions. The code is developed at AEA Culham Laboratory (UK). The model is transient and one-dimensional, although this may be planar, cylindrical, spherical or any user-specified slowly varying shape⁹¹.

It is considered that a shock wave propagates through a mixture consisting of melt droplets, water and steam. Behind the pressure front, the droplets are fragmented, and the water is heated by energy transfer from the fragments. The model assumes that this configuration can be represented using three different components: melt droplets, melt fragments and water. It is postulated that steam and water are always in mechanical and thermal equilibrium. Each species have its own velocity field.

Two different models of fragmentation are available. The first is the hydrodynamic fragmentation model; the fragmentation is due to the boundary layer stripping. The second is thermal fragmentation based model in which the fragmentation is assumed take place after a lag time since the vapor film collapse, and the rate of fragmentation is determined by a fragmentation time scale. Both the lag time and the fragmentation time scale are parametrically determined. The fragment size is also a calculation parameter, referring to the experimental data.

The heat transfer from the melt fragment to water is given either by a constant heat transfer coefficient or by a simple formulation expressing the heat transfer

coefficient as a function of the local water density.

The sensitivity study had been performed. The model predictions very sensitive to the assumed heat transfer rate. The dependence to the initial drop size and the fragment size is not significant. The author recognized the approximate nature of a number assumptions and the need further works.

3.14 ESPROSE.m Code

The ESPROSE code, developed at University California of Santa Barbara (USA), is a computational model to analyze the propagation phase in a steam explosion occurring during fuel-coolant interactions. The code is basically developed from thermal detonation concept. The original ESPROSE code was based on a three-fluid (three-field) formulation. The three fluids are fuel particles, steam and water-debris mixture⁹². Then, the code is expanded, called ESPROSE.a, by introducing the consideration of thermal fragmentation and direct vapor production⁹³. The latest development of the ESPROSE code is ESPROSE.m where the microinteraction concept is implemented (m stands for microinteraction)⁹⁴. The development from one-dimensional to three-dimensional calculation is also performed.

There are four phases: namely, 'microinteraction' fluid (m-fluid), coolant fluid (or m-external field, i.e. coolant liquid which is far from microinteraction zone), fuel melt drops, and fuel debris. The fuel debris, which is a part of microinteraction field, is assumed in thermal and hydrodynamic equilibrium with m-fluid. So, there are three velocity fields in the formulation of the conservation of momentum, i.e. m-fluid, the liquid coolant, and fuel drops.

The m-fluid is treated as a 'pseudo' gas, and the interfacial exchanges of momentum is given in the work of Medhekar et al.⁹², which is similar to flow regime map used in PM-ALPHA. The fragmentation rate is based on the instantaneous Bond number formulation⁹¹. In the model, the mass transfer between the m-fluid and liquid is considered, and is assumed to be proportional to the fragmentation rate with an empirical entrainment factor defined parametrically.

The ESPROSE.m has been verified by either analytical tests or experimental results⁹⁵. The experimental data used for comparisons are SIGMA experiments and KROTOS experiments (KROTOS-38). For the last, the PM-ALPHA code is used to provide the initial conditions of premixture.

4. SUMMARY

The recent experimental studies and code developments on premixing and propagation phases of fuel-coolant interactions are summarized in table 12 and table 13.

The experimental studies could be distinguished by the form of the hot material, i.e. the solid spheres, the melt droplets, and the melt jet. The experiments using the solid spheres, which provide a well-defined jet, are aimed to support the analytical studies (code development) of the premixing independently to the fragmentation model. The experimental results are useful for the improvement of the constitutive laws, such as the drag laws. Experiments using prototypical materials and involving large quantity have been performed in order to better simulate the real conditions. When the molten material is used, the prototypical material (i.e. $\text{UO}_2\text{-ZrO}_2$) is preferable to simulate the real condition. In this context, it is generally accepted that the material properties play an important role in the fragmentation process. It could be observed, for example, from the experiments using alumina (Al_2O_3) and corium ($\text{UO}_2\text{-ZrO}_2$). The experiments involving large quantity of melt are also performed, e.g. FARO and KROTOS experiments.

The experimental results have provided valuable data for the validation of the FCI codes being in development. However, concerning certain aspects of the physics governing the process, such as jet breakup and the drops fragmentation, the interpretation remains divers.

The development of the thermal-hydraulic codes for analyzing fuel-coolant interaction has significantly advanced recently. The codes are become more and more sophisticated. Though, lacking certain aspects of fundamental physics, various models are implemented, and a number of empirical constants are still used in the codes.

The code validation against the experiments show the spread results, as could be seen, for example, in ISP-39 on FARO Test L-14⁹⁶.

5. CONCLUDING REMARKS

The study on the premixing and propagation phases of fuel-coolant interactions has been pursuing, either in experimental or analytical works. The significant achievements have been identified. However, there is still no sufficiently validated codes, which are based on mechanistic models. For that reason, the support of sufficiently detailed experimental data is required in order to better

understanding the physics of fundamental aspects. Some innovations in the experimental technique, for example the visualization of the mixture during interaction, are encouraged. In this context, the attempt of Mishima et al.⁹⁷ to visualize molten metal-water interaction by using neutron radiography is an important path.

ACKNOWLEDGEMENT

The first author would like to gratefully acknowledge Science and Technology Agency (STA) of Japan for giving an opportunity to perform the work through Scientist Exchange Program.

REFERENCES

1. G. Long, Explosion of Metal Aluminum in Water: Cause and Prevention, Metal Progress, 71, pp. 107 – 112, 1957.
2. H.M. Factory Inspectorate UK, The Explosion at the Appleby-Frodingham Steelworks Scunthorpe November 4 1975, Report of Health and Safety Executives, 1975.
3. R.C. Reid, Rapid Phase Transitions from Liquid to Vapor, Advanced Chemical Engineering, 12, pp. 105 – 208, 1983.
4. S.A. Colgate and T. Sigurgeirsson, Dynamic Mixing of Water and Lava, Nature, 244, pp. 552 – 555, 1973.
5. G.A. Valentine, Role of Magma-Water Interaction in Very Large Explosive Eruptions, Proceedings of the International Seminar on the Physics of Vapor Explosions, October 25-29, Tomakomai (Japan), pp. 210 – 216, 1993.
6. A.W. Cronenberg, Recent Development in the Understanding of Energetic Molten Fuel – Coolant Interactions, Nuclear Safety, 21 (3), pp. 317 – 337, 1980.
7. M.L. Corradini et al., Vapor Explosion in Light Water Reactors; A Review of Theory and Modeling, Progress in Nuclear Energy, Vol. 22, No. 1, pp. 1 – 117, 1988.
8. M.L. Corradini, Vapor Explosions: A review of Experiments for Accidental Analysis, Nuclear Safety, Vol. 32, No. 3, pp. 337 – 362, 1991.
9. D.F. Fletcher, A review of the Available Information on the Triggering Stage of a Steam Explosion, Nuclear Safety, Vol. 35, No. 1, pp. 36 – 57, 1994.
10. K. Moriyama et al., Overview of Experimental Studies on Vapor Explosions, JAERI-Review 94-010, 1994. (in Japanese)
11. H.S. Park et al., Reviews of Experimental Studies on Various Geometrical Contact Modes in Vapor Explosions, JAERI-Review 96-018, 1996.
12. E.P. Hicks and D.C. Menzies, Theoretical Studies on the Fast Reactor Maximum Accident, Proc. Of the Conf. On Safety, Fuel, and Core Design in Large Fast Power Reactors, ANL-7120, pp. 654 – 670, 1965.
13. A.N. Hall, A New Thermodynamic Model of Energetic Molten Fuel-Coolant Interactions, SRDR-384, UKAE (United Kingdom), 1987.
14. L.S. Nelson et al., Photographic Evidence for the Mechanism of Fragmentation of a Single Drop of Melt in Triggered Steam Explosion Experiments, Journal of Non-equilibrium Thermodynamic, vol. 13, pp. 27-55, 1988.

15. U.S. Nuclear Regulatory Commission, A Reassessment of the Potential for an Alpha-mode Containment Failure and a Review of the Current Understanding of Broader Fuel-Coolant Interaction Issues, NUREG-1524, 1996.
16. T.P. Speis and S. Basu, Fuel-Coolant Interaction (FCI) Phenomena in Reactor Safety: Current Understanding and Future Research Needs, Proceeding of the OECD/CSNI Specialist Meeting on Fuel Coolant Interactions, Tokai-mura, Japan, May 19 – 21, JAERI-Conf 97-011, pp. 23-34, 1997.
17. H.K. Fauske, On the Mechanism of Uranium Dioxide-Sodium Explosive Interactions, Nuclear Science and Engineering, 51 (2), pp. 95-101, 1975.
18. D.H. Cho et al., Some Aspects of Mixing in Large-Mass, Energetic Fuel-Coolant Interactions, Proceedings of the 3rd Specialist Meeting on Sodium-Fuel Interaction in Fast Reactors, CONF-760328-P2 (PNC-N-251-76-12 (Vol.2), 1976.
19. M.L. Corradini, Molten fuel/coolant Interactions: Recent Analysis of Experiments, Nuclear Science and Engineering, 86, pp. 372-387, 1984.
20. T.G. Theofanous et al., "Steam Explosion : Fundamental and Energetic Behavior", NUREG/CR-5960, 1994.
21. S. Angelini et al., "Premixing – Related Behavior of Steam Explosions", Nuclear Engineering and Design, 155 (1-2), 115, 1995.
22. S. Angelini et al., "The mixing of Particle Clouds Plunging Into Water", Proceeding of the 7th International Topical Meeting on Nuclear Reactor Thermal-hydraulics, NURETH-7, NUREG/CP-0142, September 1995.
23. S. Angelini et al., "On the Regime of Premixing", Proceeding of the OECD/CSNI Specialist Meeting on Fuel Coolant Interactions, Tokai-mura, Japan, May 19 – 21, JAERI-Conf 97-011, 1997.
24. L. Meyer, " QUEOS, an Experimental Investigation of the Premixing Phase with Hot Spheres", Proceeding of the OECD/CSNI Specialist Meeting on Fuel Coolant Interactions, Tokai-mura, Japan, May 19 – 21, JAERI-Conf 97-011, 1997.
25. G. Berthoud et al., Corium – Water Interaction Studies in France, Proc. International Conference on Heat and Mass Transfer in Severe Reactor Accident, Cesme (Turkey), May 21-26, 1995.
26. G. Berthoud et al., "Premixing of Corium into Water During a Fuel-Coolant Interaction : The Models used in the 3 Fields Version of the MC3D Code and

- Two Examples of Validation on BILLEAU and FARO Experiments", Proceeding of the OECD/CSNI Specialist Meeting on Fuel Coolant Interactions, Tokai-mura, Japan, May 19 – 21, JAERI-Conf 97-011, 1997.
27. M.K. Denham et al., "Experiments on the Mixing of Molten Uranium Dioxide with Water and Initial Comparisons with CHYMES Code Calculation", Proceeding of 5th International Topical Meeting on Nuclear Reactor Thermal-hydraulics, NURETH-5, Salt Lake City, UT, September 21 – 24, 1992.
 28. A. Kaiser et al., "Melt Water Interaction Tests (PREMIX Tests PM10 and PM11)", Proceeding of the OECD/CSNI Specialist Meeting on Fuel Coolant Interactions, Tokai-mura, Japan, May 19 – 21, 1997.
 29. J. Sugimoto, "Overview of Severe Accident Research at JAERI", Proceedings of the Workshop on Severe Accident Research in Japan, SARJ-97, Tokyo, Japan, Oct. 6 – 8, JAERI-Conf 98-009, 1997.
 30. J. Sugimoto et al., "Fuel – Coolant Interaction Experiments in ALPHA Program", Proceeding of International Topical Meeting on Nuclear Reactor Thermal-hydraulic, NURETH-5, Salt Lake City, UT, September 21 – 24, 1992.
 31. N. Yamano et al., Assessment of Loads and Performance of a Containment in a Hypothetical Accident (ALPHA): Facility Design Report, JAERI-Tech 98-019, 1998. (in Japanese)
 32. N. Yamano et al., "Phenomenological Studies on Melt – Coolant Interactions in the ALPHA Program", Nuclear Engineering and Design, 155 (1-2), 369, 1995.
 33. H.S. Park et al. Design and First Integral Test of MUSE Facility in ALPHA Program, JAERI-Tech 98-007, 1998.
 34. N. Yamano et al., "Study on Premixing Phase of Steam Explosion at JAERI", Proceeding of the OECD/CSNI Specialist Meeting on Fuel Coolant Interactions, Tokai-mura, Japan, May 19 – 21, JAERI-Conf 97-011, 1997.
 35. D. Magalon and H. Hohmann, "High Pressure Corium Melt Quenching Test in FARO", Nuclear Engineering and Design, 155 (1-2), pp. 253 – 270, 1995.
 36. D. Magalon and H. Hohmann, "Experimental Investigation of 150 kg Scale Corium Melt Jet Quenching in Water", Proceeding of the 7th International Topical Meeting on Nuclear Reactor Thermal-hydraulics, NURETH-7, NUREG/CP-0142, September 1995.
 37. D. Magalon et al., "Lessons Learnt from FARO/TERMOS Corium Melt

- Quenching Experiments", Proceeding of the OECD/CSNI Specialist Meeting on Fuel Coolant Interactions, Tokai-mura, Japan, May 19 – 21, JAERI-Conf 97-011, 1997.
38. C. Addabbo et al., "Synopsis of the Results of ISP-39 on FARO Test L-14", Proceeding of the OECD/CSNI Specialist Meeting on Fuel Coolant Interactions, Tokai-mura, Japan, May 19 – 21, JAERI-Conf 97-011, 1997.
 39. D.E. Mitchell et al., Intermediate-scale Steam Explosion Phenomena: Experiments and Analysis, NUREG/CR-2145, 1981.
 40. M.J. Bird, An Experimental Study of Scaling in Core Melt/water Interactions, 22nd National Heat Transfer Conference, Niagara Falls (USA), 1984.
 41. S.J. Board et al., Detonation of fuel coolant explosions, *Nature*, 254, pp. 319-321, 1975.
 42. R.W. Hall and S.J. Board, The Propagation of Large Scale Thermal Explosion, *International Journal of Heat and Mass Transfer*, 22, pp. 1083-1093, 1979.
 43. D.F. Fletcher and R.P. Anderson, A Review of Pressure-Induced Propagation Models of the Vapor Explosion Process, *Progress in Nuclear Energy*, 23(2), pp. 137-179, 1990.
 44. X. Chen et al., On the Constitutive Description of the Microinteractions Concepts in Steam Explosions, Proceedings of 7th International Meeting on Nuclear Reactor Thermal-Hydraulics (NURETH-7), New York (USA), September 10-15, pp. 1586-1606, 1995.
 45. X. Chen et al., Experimental Simulation of Microinteractions in Large Scale Explosion, Proc. Of the OECD/CSNI Specialists Meeting on Fuel-Coolant Interactions, Tokai-mura (Japan), May 19-21, JAERI-Conf 97-011, 1997.
 46. G. Fröhlich, Propagation of fuel-coolant Interactions in Multi-jet experiments, Proceedings 4th International Topical Meeting on Nuclear Reactor Thermal-hydraulics, Karlsruhe (Germany), October 10-13, pp.282-289, 1989.
 47. G. Fröhlich, Propagation of fuel-coolant Interactions in Multi-jet experiments with molten Tin, *Nuclear Engineering and Design*, 131, pp. 209-221, 1991.
 48. H. Hohmann et al., Fuel-Coolant Interaction Experiments in the Aluminum Oxide/Water System, *Nuclear Engineering and Design*, 155, pp. 391-403, 1995.
 49. I. Huhtiniemi, et al., "Fuel – Coolant Interaction Experiments in the Corium/Water System", Proceeding of the 7th International Topical Meeting on Nuclear Reactor Thermal-hydraulics, NURETH-7, NUREG/CP-0142, Vol.

- 3, pp. 1712 – 1727, September 1995.
50. I. Huhtiniemi, et al., "Results of Recent KROTOS Fuel – Coolant Interaction Tests", Proceeding of the OECD/CSNI Specialist Meeting on Fuel Coolant Interactions, Tokai-mura, Japan, May 19 – 21, JAERI-Conf 97-011, 1997.
 51. F.K. Davis and M.F. Young, Integrated Fuel-Coolant Interaction (IFCI 6.0) Code, NUREG/CR-6211, SAND94-0406, 1994.
 52. M.F. Young, IFCI: An integrated Code for Calculation of All Phases of Fuel-Coolant Interactions, NUREG/CR-5084, SAND87-1048, 1987.
 53. C.C. Chu et al., A Code Manual for TEXAS-V: One Dimensional Transient Fluid Model Fuel-Coolant Interaction Analysis, revision June 1996, <http://silver.neep.wisc.edu/~NSRC/texas>, 1998.
 54. M.F. Young, The TEXAS Code for Fuel-Coolant Interaction Analysis, Liquid Metal Fast Breeder Reactor Safety Topical Meeting, Lyon (France), 1982.
 55. C.C. Chu and M.L. Corradini, "One-dimensional Transient Model for Fuel-Coolant Interaction Analysis", Nuclear Science Engineering, Vol. 101, 1989.
 56. J. Tang and M.L. Corradini, Modeling of the Complete Process of One-Dimensional Vapor Explosion, Proceedings of the CSNI Specialists Meeting on Fuel-Coolant Interactions, Santa Barbara (USA), January 5-8, pp. 204-217, 1993.
 57. M.L. Corradini et al., "Fuel Fragmentation Model Advances Using TEXAS-V", Proceeding of the OECD/CSNI Specialist Meeting on Fuel Coolant Interactions, Tokai-mura, Japan, May 19 – 21, JAERI-Conf 97-011, 1997.
 58. D.F. Fletcher and A. Thyagaraja, The CHYMES Coarse Mixing Model, Progress in Nuclear Energy, 26, 1, pp. 31-61, 1991.
 59. M.K. Denham et al., Experiments on the Mixing of Molten Uranium Dioxide With Water and Initial Comparisons with CHYMES code calculations, Nuclear Engineering and Design, 146, pp. 97-108, 1994.
 60. W.H. Amarasooriya and T.G. Theofanous, Premixing of Steam Explosions: a Three-fluid Model, Nuclear Engineering and Design, 126, pp. 23-39, 1991.
 61. S. Angelini et al., Multiphase Transients in the Premixing of Steam Explosions, Nuclear Engineering and Design, 146, pp. 83-95, 1994.
 62. T.G. Theofanous et al., The Verification Basis of the PM-ALPHA Code, Proceeding of the OECD/CSNI Specialist Meeting on Fuel Coolant Interactions, Tokai-mura, Japan, May 19 – 21, JAERI-Conf 97-011, pp. 219-268, 1997.
 63. G. Berthoud and M. Valette, "Development of Multidimensional Model for the

- Premixing Phase of Fuel – Coolant Interaction”, Nuclear Engineering and Design, 149, 409 - 418, 1994.
64. G. Berthoud et al., “Premixing of Corium into Water During a Fuel-Coolant Interaction : The Models used in the 3 Fields Version of the MC3D Code and Two Examples of Validation on BILLEAU and FARO Experiments”, Proceeding of the OECD/CSNI Specialist Meeting on Fuel Coolant Interactions, Tokai-mura, Japan, May 19 – 21, JAERI-Conf 97-011, 1997.
 65. G. Berthoud et al., “ Description of Premixing with the MC3D Code Including Molten Jet Behavior Modeling, Comparison with FARO Experimental Results”, Proceeding of the OECD/CSNI Specialist Meeting on Fuel Coolant Interactions, Tokai-mura, Japan, May 19 – 21, JAERI-Conf 97-011, 1997.
 66. C. Brayer and G. Berthoud, “ First Vapor Explosion Calculation Performed with MC3D Thermal-hydraulic Code”, Proceeding of the OECD/CSNI Specialist Meeting on Fuel Coolant Interactions, Tokai-mura, Japan, May 19 – 21, JAERI-Conf 97-011, 1997.
 67. K. Moriyama et al., FCI Simulation Code Development in ALPHA Program, Proceedings of Seminar on the Vapor Explosions in Nuclear Power Safety, Izu (Japan), pp. 150-159, 1996.
 68. K. Moriyama et al., Development of Steam Explosion Simulation Code JASMINE, JAERI-Data/Code 95-016, 1995 (in Japanese).
 69. K. Moriyama et al., Study of Premixing Phase of Steam Explosion with JASMINE code in ALPHA Program, Proceedings of 4th International Conference on Nuclear Engineering, ICON-4, New Orleans (USA), pp. 903-915, 1996.
 70. K. Moriyama et al., Development and Validation of JASMINE Code in ALPHA Program, presented at the Workshop on Severe Accident Research in Japan, Tokyo(Japan), October 28-30, 1996.
 71. K. Vierow et al., Development of the VESUVIUS Model and Analysis of the Premixing Phase of An Ex-Vessel Steam Explosion, Proceedings of 4th International Conference on Nuclear Engineering (ICON-4), pp. 333-341, 1996.
 72. K. Vierow, Development of the VESUVIUS Module for Analysis of Ex-Vessel Steam Explosions, Proceedings of Seminar on the Vapor Explosions in Nuclear Power Safety, Izu (Japan), July 8-10, pp. 160-173, 1996.
 73. K. Vierow et al., “Development of the VESUVIUS Module : Molten Jet Breakup Modeling and Model Verification, Proceeding of the OECD/CSNI

- Specialist Meeting on Fuel Coolant Interactions, Tokai-mura, Japan, May 19 – 21, JAERI-Conf 97-011, 1997.
74. J.J. Sienicki et al., Ex-Vessel Melt-Coolant Interactions in Deep Water Pool: Studies and Accident Management for Swedish BWRs, Proceedings of the CSNI Specialist Meeting on Fuel-Coolant Interactions, Santa Barbara (USA), January 5-8, pp. 37-54, 1993.
 75. J.J. Sienicki et al., Analysis of Melt Arrival Conditions on the Lower Head in US LWR Configurations, Proceedings of the 5th International Topical Meeting on Reactor Thermal Hydraulic (NURETH-5), Salt Lake City, September 21-24, pp. 450-, 1992.
 76. C.C. Chu et al., Ex-vessel Melt-Coolant Interactions in Deep Water Pool: Studies and Accident Management for Swedish BWRs, Nuclear Engineering and Design, 155, pp. 159-213, 1995.
 77. C.C. Chu et al., Comparison of THIRMAL-1 Predictions with FARO and CCM Experiments, Transactions of the ANS, Vol. 71, 1994.
 78. E.v. Berg et al., Modeling of the Breakup of Melt Jets in liquids for LWR safety Analysis, Nuclear Engineering and Design, 149, pp. 419-429, 1994.
 79. M. Burger et al., "Breakup of Melt Jets as Pre-condition for Premixing Modeling and Experimental Verification", Nuclear Engineering and Design, 155 (1-2), 215, 1995.
 80. M. Burger et al., Consideration and Calculations on the Breakup of Jets and Drops of Melt related to Premixing, Proceeding of the OECD/CSNI Specialist Meeting on Fuel Coolant Interactions, Tokai-mura, Japan, May 19 – 21, JAERI-Conf 97-011, 1997.
 81. A. Annunziato and C. Addabbo, COMETA (Core Melt Thermal-hydraulic Analysis) a Computer Code for Melt Quenching Analysis, Proceeding of International Conference on New Trends in Nuclear System Thermal-hydraulics, Pisa (Italy), May 30 – June2, pp. 391-406, 1994.
 82. A. Annunziato et al., FARO and KROTOS Code Simulation and Analysis at JRC-Ispra, Proceeding of the OECD/CSNI Specialist Meeting on Fuel Coolant Interactions, Tokai-mura, Japan, May 19 – 21, JAERI-Conf 97-011, 1997.
 83. K.H. Bang et al., TRACER-II: A Complete Computational Model for Mixing and Propagation of Vapor Explosions, Proceeding of the OECD/CSNI Specialist Meeting on Fuel Coolant Interactions, Tokai-mura, Japan, May 19 – 21, JAERI-Conf 97-011, 1997.

84. H. Jacobs and L. Meyer, Highly Transient and Intense Multiphase Interactions in The QUEOS Premixing Experiments, Proceedings of the International Seminar on Vapor Explosions and Explosive Eruptions, Sendai (Japan), May 22-25, pp. 253-262, 1997.
85. N.I. Kolev, The Code IVA4: Modeling of Mass Conservation in Multi-phase Multi-component flows in Heterogeneous Porous Media, Kerntechnik 59, No. 4-5, pp. 226-237, 1994.
86. N.I. Kolev, The Code IVA4: Modeling of Momentum Conservation in Multi-phase Multi-component flows in Heterogeneous Porous Media, Kerntechnik 59, No. 6, pp. 249-258, 1994.
87. H. Jacobs et al., Constitutive Relations for Multiphase Flow Modeling, Proceeding of the OECD/CSNI Specialist Meeting on Fuel Coolant Interactions, Tokai-mura, Japan, May 19 – 21, JAERI-Conf 97-011, pp. 205-217, 1997.
88. H. Jacobs et al., Constitutive Relations for Multiphase Flow Modeling, Proceeding of the OECD/CSNI Specialist Meeting on Fuel Coolant Interactions, Tokai-mura, Japan, May 19 – 21, JAERI-Conf 97-011, pp. 205-217, 1997.
89. N.I. Kolev, IVA4 Analysis of the FARO I-14 Experiment, Proceedings of the International Seminar on Vapor Explosions and Explosive Eruptions, Sendai (Japan), May 22-25, pp. 263-272, 1997.
90. N.I. Kolev, Numerical Modeling of IN-vessel Melt Water Interaction in Large Scale PWR's, Proceeding of the OECD/CSNI Specialist Meeting on Fuel Coolant Interactions, Tokai-mura, Japan, May 19 – 21, JAERI-Conf 97-011, pp. 145-149, 1997.
91. D.F. Fletcher, Propagation Investigation Using the CULDESAC Model, Nuclear Engineering and Design, 155, pp. 271-287, 1995.
92. S. Medhekar et al., Integrated Analysis of Steam Explosions, Proceedings of the 4th International Topical Meeting on Nuclear Reactor Thermal-Hydraulics (NURETH-4), Karlsruhe (Germany), pp. 319-326, 1989.
93. W.W. Yuen et al., On the Fundamental Microinteractions that Support the Propagation of Steam Explosion, Nuclear Engineering and Design, 146, pp. 133-146, 1994.
94. W.W. Yuen and T.G. Theofanous, The Prediction of 2D Thermal Detonation and Resulting Damage Potential, Nuclear Engineering and Design, 155, pp. 289-309, 1995.

95. T.G. Theofanous et al., The Verification Basis of the ESPROSE.m Code, Proceeding of the OECD/CSNI Specialist Meeting on Fuel Coolant Interactions, Tokai-mura, Japan, May 19 – 21, pp. 287-362, 1997.
96. A. Annunziato et al., OECD/CSNI International Standard Problem 39 on FARO Test L-14 on Fuel Coolant Interaction and Quenching: Analysis of the Results, EUR 17736 EN, 1998.
97. K. Mishima et al., Visualization Study of Molten Metal-Water Interaction by Using Neutron Radiography, Proceedings of International Seminar on Vapor Explosions and Explosive Eruptions, Sendai (Japan), May 22-24, pp. 45-101-110, 1997.

Table 1 Specification of the cold runs²²

Run#	Particulate	Size Range (mm)	Total Mass (kg)	Plunging Velocity (m/s)	Inlet Volume Fraction (%)	Cloud Length/ Diameter (cm)	Pool Geometry/ Depth (cm)
MA.AX	Al ₂ O ₃	1.5-2.5	5.4	5.0	9.4	43/22.0	60x60/60
MA.CR	Al ₂ O ₃	1.5-2.5	5.4	5.0	9.4	43/22.0	60x30/60
MZ.AX	ZrO ₂	2.4-3.4	8.6	5.0	10.9	37/22.0	60x60/60
MZ.CR	ZrO ₂	2.4-3.4	8.6	5.0	10.9	37/22.0	60x30/60
MZD.AX	ZrO ₂	2.4-3.4	8.6	4.0	10.9	37/22.0	60x60/120
MF.AX	Steel	2.4	12.2	5.0	13.3	37/22.0	60x60/60
MF.CR	Steel	2.4	12.2	5.0	13.3	37/22.0	60x30/60

Table 2 Specification of the hot runs²²

Run	Particulate/ Size Range (mm)	Total Mass (kg)	Pour Diameter (cm)	Pour Duration (s)	Plunging Velocity (m/s)	Inlet Volume Fraction (%)	Particle Temperature (°C)	Water Subcooling/ Depth (°C/cm)
ZI500/0-1	ZrO ₂ /2.4-3.4	6.2	22.5	0.33	5.0	1.71	1300-1450	0/60
ZI500/0-2	ZrO ₂ /2.4-3.4	6.2	22.5	0.33	4.8	1.71	1300-1450	0/80
ZI500/3-4	ZrO ₂ /2.4-3.4	8.0	22.5	0.33	4.8	2.21	1300-1450	3/80
ZI500/18-5	ZrO ₂ /2.4-3.4	8.6	22.5	0.33	4.8	2.38	1300-1450	18/80
SI200/0-6	SiC/1.0-4.0	2.85	22.0	0.33	4.8	1.46	1150-1200	0/80

Table 3 Conditions for the Cold MAGICO-2000 run in 2D slab geometry²³

Run	Particle Size (mm)	Total Mass (kg)	Volume Fraction (%)	Impact Velocity (m/s)
ZCN	2	5.5	~6.5	~5.2
ZCT	7	5.0	~0.5	~4.4

Table 4 Conditions for the hot MAGICO-2000 runs in 2D slab geometry²³

Run	Particle Size (mm)	Total Mass (kg)	Volume Fraction (%)	Impact Velocity (m/s)	Particle Temperature (°C)	Water Subcooling (°C)
Z11	2	5.5	4.2	5.2	1500	0
Z12	2	5.7	4.2	5.2	1400	10
Zb13	7	4.8	5.5	5.2	1600	0
ZT14	7	5.1	0.5	4.4	1650	0
ZT15	7	4.4	0.5	4.4	1800	0
ZT16	7	2.6	0.5	4.4	2000	0

Table 5 Initial Conditions of QUEOS Hot Spheres Experiments²⁴

No.	Mat'l	Size (mm)	Mass (kg)	Volume (cm ³)	Number of spheres	Water temp. (°C)	Sphere temp. in furnace ±5(°C)	Furnace temp. ± 20(°C)	Sphere temp. above water ±40 (°C)	Duration of Pour ±5 (ms)	Length of pour ± 3 (cm)	Average volume fraction ±0.01
30	ZrO ₂	4.95	7	1830	18140	80.4	1535	1561	1550	125	62	0.24
31	ZrO ₂	4.95	7	1830	18140	99.0	1558	1683	1570	115	57	0.26
32	ZrO ₂	4.95	14	3660	36280	98.5	1545	1665	1620	220	110	0.27
33	ZrO ₂	9.80	7	1900	2340	98.7	1572	1664	1600	115	57	0.26
34B	ZrO ₂	9.80	14	3800	4680	99.0	1542	1642	1600	250	125	0.24
35	Mo	4.32	10	1800	24580	98.4	1517	1586	1540	125	62	0.22
36	Mo	4.32	20	3600	49160	98.3	1539	1563	1550	220	110	0.24

Table 6 Initial conditions of First Test Series of BILLEAU²⁵

TEST #	FPD37	FPD40	FPD98	FPA39	FPA96	FPA97
<i>Sphere</i>						
Material	DURAL	DURAL	DURAL	SS	SS	SS
Density (kg/m ³)	2.7x10 ³	2.7x10 ³	2.7x10 ³	7.8 x10 ³	7.8 x10 ³	7.8 x10 ³
Diameter (cm)	0.952	0.5	0.952	0.5	0.952	0.952
Total Number	360	320	720	360	720	720
<i>Tubes</i>						
Number	4	6	8	6	8	8
Internal Diameter (m)	10.x10 ⁻³	6.x10 ⁻³	10.x10 ⁻³	6. x10 ⁻³	10.x10 ⁻³	10.x10 ⁻³
Fall Height (m)	0.10	0.10	0.10	0.10	0.10	0.10
<i>Test Section</i>						
Water depth (m)	0.9	0.9	0.9	0.9	0.9	0.9
Thickness (m)	12 x10 ⁻³	12 x10 ⁻³	12 x10 ⁻³	1.5	12 x10 ⁻³	12 x10 ⁻³

Table 7 Experimental conditions and main results²⁷

Experiments	MIXA01	MIXA02	MIXA03
Melt mass (kg)	2.84	2.75	3.00
Skirt length (m)	No skirt	210	480
Melt volume fraction	0.01	0.015	0.03
Time to penetrate – 200 mm (ms)	470	240	210
Time to penetrate – 600 mm (ms)	600	520	480
Steam Volume (m3)	1.286	1.067	0.701

Table 8. Test Run Conditions of ALPHA MJB³³

EXPERIMENT	MJB01	MJB02
Melt Initial Mass (g)	19840	20000
Melt Initial Temperature (K)	475	483
Ambient Pressure (MPa)	0.1	0.1
Melt Jet Diameter (mm)	30	21
Melt Jet Initial Velocity (m/s)	3.05	2.86
Water Temperature (K)	373	373

Table 9 Main data of FARO tests³⁶

No	Parameters	Test No.						
		L-06	L-08	L-11*	L-14	L-19	L-20	L-24
1.	Initial pressure (MPa)	5.0	5.8	5.0	5.0	5.0	2.0	0.5
2.	Melt mass (kg)	18	44	151	125	157	96	176
3.	Melt temperature (K)	2923	3023	2823	3073	3073	3173	3023
4.	Melt free fall in gas (m)	1.66	1.53	1.09	1.04	1.99	1.12	1.07
5.	Water depth (m)	0.87	1.00	2.00	2.05	1.10	1.97	2.02
6.	Melt leading edge velocity (m/s)	2.3	3.7	2.5/1.2	4.8	4.2	3.3	3.8
7.	Cake on bottom (kg)	6	14	0	20	80	21	
8.	Particulate debris (kg)	12	30	151	105	77	75	
9.	Mean Particle size (mm)	4.5	3.8	3.5	4.8	3.7	4.4	

*Melt composition : 76.7 w% UO₂ + 19.2 w% ZrO₂ + 4.1 w% Zr

Table 10 Initial conditions and main test results of alumina tests series⁵⁰.

KROTOS TEST No.		38	40	41	42	43	44	49	50	51
Melt	Loaded mass (g)	1533	1470	1430	1539	1500	1500	1470	1700	1794
	Temperature (K)	2665	3073	3073	2465	2625	2673	2688	2473	2748
	Superheat (K)	351	759	759	151	311	359	374	159	434
	Thermal energy (kJ)	6285	6870	6473	5124	6065	6166	6074	6036	7423
Water	Mass (kg)	34.1	34.8	36.0	34.8	34.8	35.6	34.8	35.7	36.0
	Bulk temperature (K)	294	290	368	293	295	363	294	360	368
	Subcooling (K)	79	83	5	80	100	10	120	13	5
Test Vessel	Initial pressure (MPa)	0.1	0.1	0.1	0.1	0.21	0.1	0.37	0.1	0.1
	Temperature (K)	291	292	328	294	296	328	298	305	324
Results Mixing	Void fraction (%)	2.6	12.1	14.2	1.0	1.9	10.4	0.6	10.6	30.2
Results Explosion	Steam explosion	Yes	Yes	No	Yes	Yes	Yes	Yes	No	No
	Max. pressurisation in t.s. (MPa)	112	86	-	57	117	68	127	-	-
	Efficiency (%)	1.52	0.87	-	2.13	1.27	2.48	2.41	-	-
Results Debris	Collected mass (g)	1525	1509*	1385	1342	1688*	1449	1735*	1576	1760
	Mass < 106 μ m (g)	545	349	0	421	458	682	648	0	73

*Larger than loaded mass due to extra debris from level meters and injection nozzle destroyed by steam explosions

Table 11 Initial conditions and main test results of corium⁵⁰.

KROTOS TEST No.		37	45	47	52
Melt	Loaded mass (g)	3222	3085	5431	2617
	Temperature (K)	3018	3106	3023	3023
	Superheat (K)	168	256	173	173
	Thermal energy (kJ)	4665	4590	8220	3884
Water	Mass (kg)	34.2	36.3	34.1	34.1
	Bulk temperature (K)	296	369	291	290
	Subcooling (K)	77	4	82	102
Test Vessel	Initial pressure (MPa)	0.1	0.1	0.1	0.2
	Temperature (K)	298	327	299	292
Results Mixing	Void fraction (%)	22.2	31.3	31.6	13.4
Results Explosion	Steam explosion	No	No	No	No
Results Debris	Collected mass (g)	2925	2791*	5145	2431
	Mass < 106 μ m (g)	41	54	358	345

Table 12 Summary of Recent FCI Experimental Works

Program/ Facility	Organization (Country)	Type	Molten Materials	Program Objectives/ Main Results
ALPHA	JAERI (Japan)	Melt jet/ Pour	Thermite Pb-Bi alloy	Investigate energetic steam explosion (pouring and injection mode of contact), coolability of melt and molten jet break up (premixing) Main results: - Various data on characteristic of different stages of a molten fuel-coolant interactions (e.g. premixing, quenching, jet breakup, explosion) on various mode of contact Investigate premixing phase with cold and hot solid spheres Main results: - Data on characteristic of plunging jet into a coolant - Observation of mushroom-like shape in front of the jet
BILLEAU	CEA/IPSN (France)	Solid spheres	DURAL, ZrO ₂	Investigate non-explosive melt-coolant interactions (quenching, breakup of molten jet) using a large quantity of prototypic melt (up to 150 kg) at a wide range of system pressures (0.5 – 5.0 MPa) in large vessel Main results: - Data on various parameters during premixing, e.g. pressurization, debris diameter, energy released - Zr metal enhances breakup and provides higher pressurization
FARO	JRC-Ispra (EU)	Melt jet	UO ₂ -ZrO ₂	Investigate explosive melt-coolant interactions (propagation phase) usually at atmospheric pressure in small vessel Main results: - Data on behavior of explosion - Al ₂ O ₃ /water: spontaneous explosion - Corium/water: no explosion, higher void fraction during mixing
KROTOS	JRC-Ispra (EU)	Melt jet	UO ₂ -ZrO ₂ Al ₂ O ₃	

Table 12 Summary of Recent FCI Experimental Works (continued)

Program/ Facility	Organization (Country)	Type	Molten Materials	Program Objectives/ Main Results
MAGICO	UCSB (USA)	Solid spheres	Steel, Al_2O_3 , ZrO_2 , SiC	Investigate premixing and water depletion phenomena using solid spheres with various volume fractions, high temperatures (2000K) Main results: - Data on characteristic of solid particles jet plunging into coolant, especially measurements of local void fractions - Observation of gas hole behind a dense cloud in front of jet - Dilute cloud: particles are distributed uniformly
MIXA	AEA- Winfrith (UK)	Stream of melt droplets	UO_2 -Mo	Investigate premixing phenomena using stream of melt droplets and to validate CHYMES code Main results: Data on premixing phase Low concentration melt experiences higher deceleration, larger spread
Multi-jet	IKE- Stuttgart (Germany)	Stream of small jets	Tin	Investigate propagation phenomena in 3D condition (in case far removed from thermal detonation condition) Main results: - Data on characteristic of propagation, propagation velocity - Explosion propagates in jump from one center to others by a shock waves - Average propagation velocity of 4m/s
PREMIX	FZK (Germany)	Melt jet	Al_2O_3	Investigate the limitation of the mass in premixing phase Main results: - Observation of explosion in case of triple jets

Table 12 Summary of Recent FCI Experimental Works (continued)

Program/ Facility	Organization (Country)	Type	Molten Materials	Program Objectives/ Main Results
QUEOS	FZK (Germany)	Solid spheres	ZrO ₂ , Mo	Investigate premixing phenomena using cold and hot solid spheres with different diameters Main results: - Observation of gas channel behind the dense front jet - Small diameter of particles produces higher pressure rise - Heavy sphere and large total mass spread less
SIGMA	UCSB (USA)	Single melt drop	Tin, steel, etc.	Investigate kinetic fragmentation of molten droplets at various shock pressure; leads to "micro-interactions concept" during propagation phase Main results: Data to validate ESPROSE.m code Stronger fragmentation in two-phase coolant

Table 13 Summary of the code overview

Code Name (organization, country)	FCI phase modeled	No. of Dim.	Velocity field	Fragmentation model	Other remarks / specific features	Experiments used for validation
IFCI (SNL, USA)	Premixing Triggering Propagation Expansion	2	Vapor (E) Liquid coolant. (E) Melt (E) Solid fuel (E)	Jet: not implemented Drop: RTI	1) Length scale of melt > grid size, melt is considered as continuous jet 2) Jet interface tracking: VOF	FITS FARO L-14
TEXAS (UW, USA)	Premixing Triggering Propagation Expansion	1	Vapor (E) Liquid coolant (E) Fuel (L)	Jet leading edge: BLS Surface of body jet: KHI Drop: RTI Pro: thermal fragmentation (K-C model)	Jet is taken as a series of discrete droplets	FARO L-14
CHYMES (AEA, UK)	Premixing	2	Vapor (E) Liquid coolant (E) Fuel (E)	Drop: RTI or simple parametric model	1) Jet is taken as agglomeration of droplets 2) Vapor and coolant liquid in saturation	BNL tests MIXA
PM-ALPHA (UCSB, USA)	Premixing	2	Vapor (E) Liquid coolant (E) Fuel (E)	No fragmentation model	1) Jet as pre – fragmented melt 2) Enhanced flow regime map	MAGICO QUEOS MIXA FARO

Table 13 Summary of the code overview (continued)

Code Name (organization)	FCI phase modeled	No. of Dim.	Velocity field	Fragmentation model	Other remarks / specific features	Experiments used for validation
MC3D (CEA, France)	Premixing Propagation	3	Vapor+n.c gas (E) Liquid coolant (E) Pre: melt jet (E) Droplet (E) Pro: Droplet (E) Debris (E)	Jet: no detailed model Drop: RTI Pro: Thermal and hydrodynamic model	1) Jet interface tracking: VOF 2) jet breakup is given by various parameters	BILLEAU FARO L-14 KROTOS
JASMINE (JAERI, Japan)	Premixing Propagation (underway)	3	Vapor (E) Liquid coolant (E) Fuel (E)	Jet: KHI Drop: RTI	1) Fuel consists of melt jet and droplets -2) Continuous jet in central node	MAGICO FARO L-14 ALPHA-MJB
VESUVIUS (NUPEC, Japan)	Premixing Propagation (underway)	3	Vapor (E) Liquid coolant (E) Melt jet (E) Droplet (E)	Jet: KHI Drop: RTI	Continuous jet in central node	MIXA FARO L-06
THIRMAL (ANL, USA)	Premixing	1	Vapor (E) Liquid coolant (E) Melt (L)	Jet: KHI breakup model Drop: No breakup model	1) Can support the presence of distinct oxide and metal in melt 2) H ₂ generation model	FARO CCM

Table 13 Summary of the code overview (continued)

Code Name (organization)	FCI phase modeled	No. of Dim.	Velocity field	Fragmentation model	Other remarks / specific features	Experiments used for validation
IKEJET (IKE-Stuttgart, Germany)	Premixing	1	Molten jet (E)	Jet: KHI Drop: no breakup model		PREMIX FARO L-14, L-20
COMETA (JRC-Ispra, EU)	Premixing	1 or 2	Two-phase (E) in 2 equations Melt (L)	Jet: L/D criteria or TEXAS model or IKEJET model Drop: We criteria	1) Two-phase field composes of liquid coolant and vapor 2) Melt consists of jet, droplets and debris 3) H ₂ generation model	FARO
TRACER-II (Korea Maritime Univ., S. Korea)	Premixing Propagation	2	Vapor (E) Liquid coolant (E) Melt (E)	Jet: RTI Pro: BLS	1) Jet is taken as stream of droplet 2) Fragmented fuel debris moves together with liquid continuum	FARO L-14 KROTOS-28
IVA-KA / IVA4 (KfK/Siemens, Germany)	Premixing	3	Vapor (E) Liquid coolant (E) Melt (E)	Jet: L/D criteria Drop: We criteria	1) no explicit jet model 2) Coalescence is modeled	QUEOS FARO

Table 13 Summary of the code overview (continued)

Code Name (organization)	FCI phase modeled	No of Dim.	Velocity field	Fragmentation model	Other remarks / specific features	Experiments used for validation
CULDESAC (AEA, UK)	Propagation	1	Coolant (E) Melt droplet (E) Melt fragments (E)	Droplet: BLS	Coolant consists of vapor and liquid in equilibrium	
ESPROSE.m (UCSB, USA)	Propagation	3	m-fluid (E) Liquid coolant (E) Melt drop (E)	Drop: hydrodynamic insta- bilities	m-fluid is micro- interaction fluid, and contains fuel debris, vapor and coolant liquid	SIGMA KROTOS-38

Note:

E : Eulerian
 L : Lagrangian
 Pre: Premixing
 Pro: Propagation
 RTI : Rayleigh-Taylor Instability
 KHI : Kelvin-Helmholtz Instability
 K-C : Kim-Corradini
 BLS : Boundary Layer Stripping
 VOF : Volume-of-Fluid
 We : Weber Number

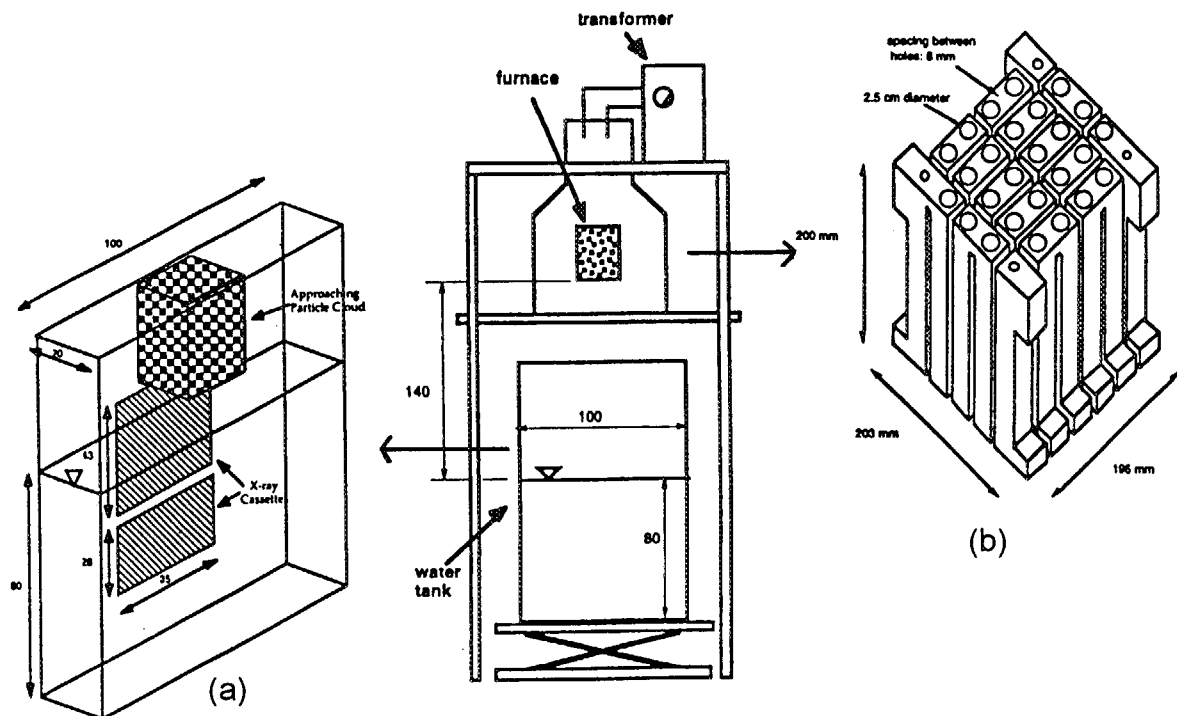


Figure 1 Schematic of MAGICO-2000 experimental facility with the interaction tank (a) and the heating element (b)

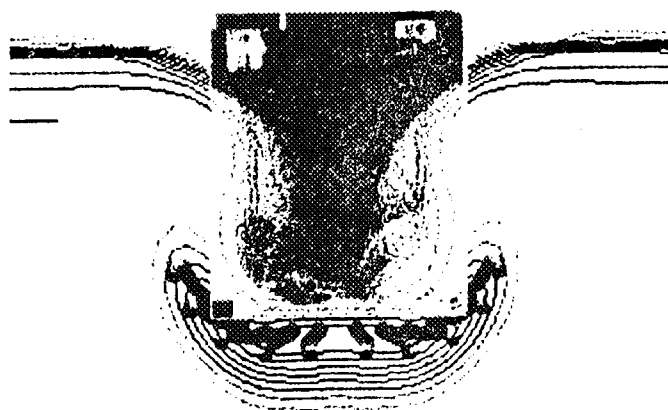


Figure 2 MAGICO-2000 experiments: superposition of X-ray radiographs and calculation results on jet contours of one cold run

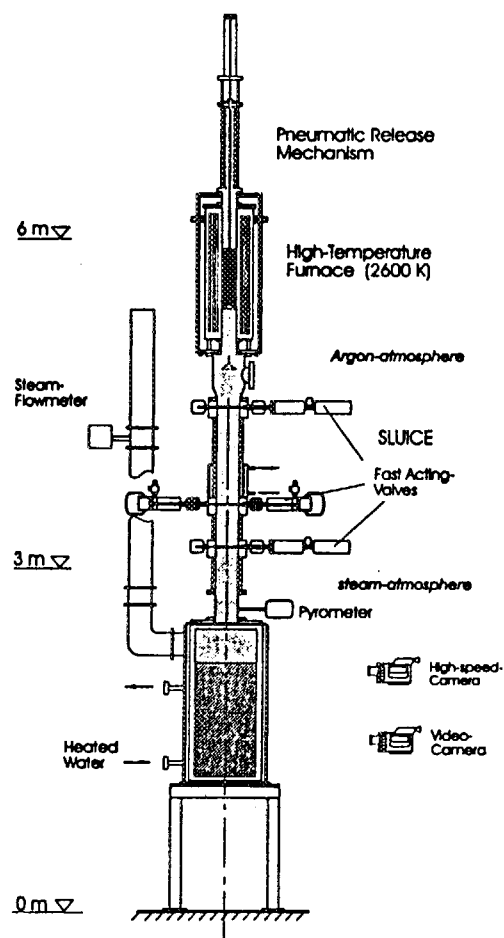


Figure 3 QUEOS Test Facility

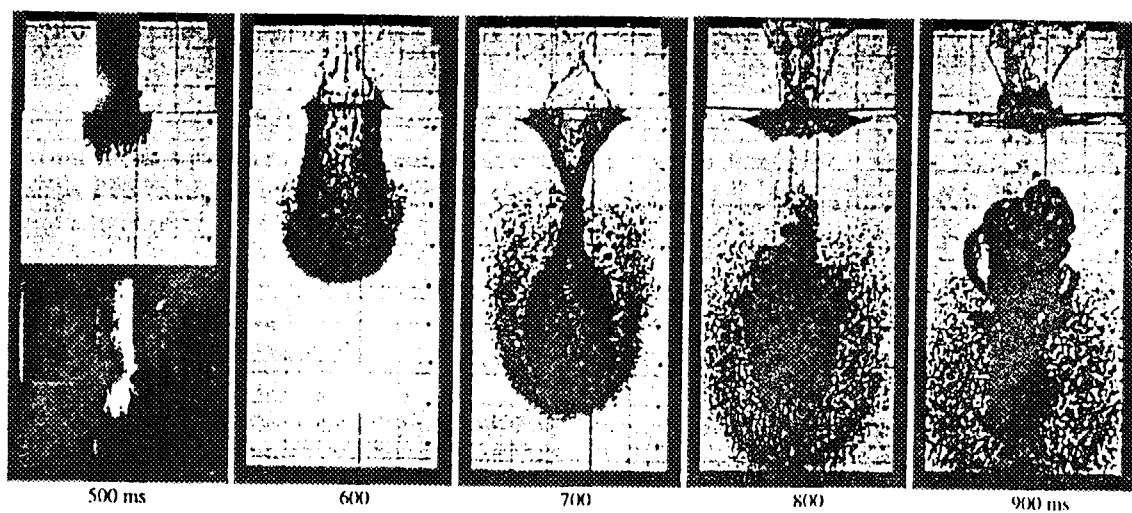


Figure 4 QUEOS test: photograph of one cold run.

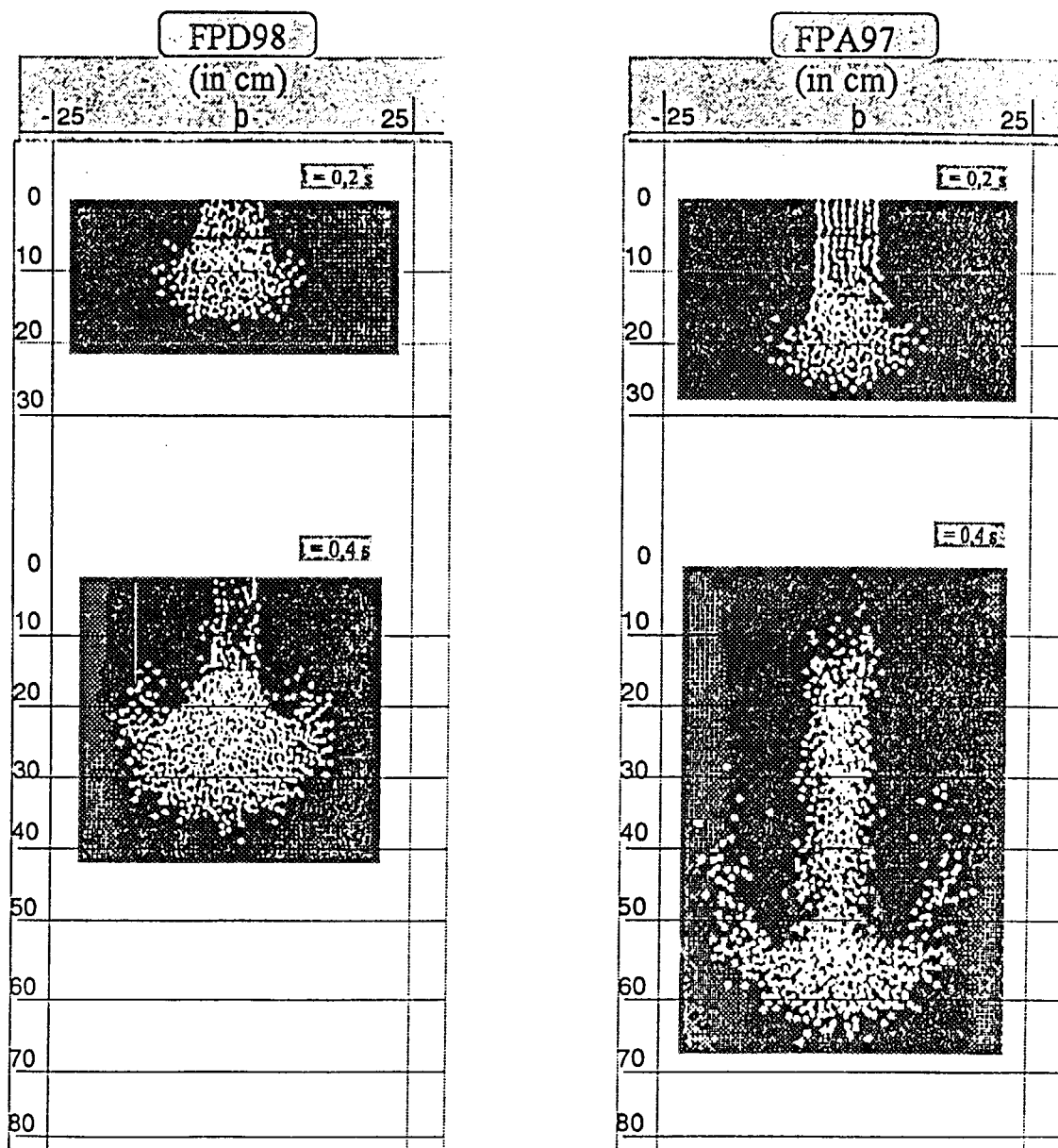


Figure 5 BILLEAU experiment: Photographs of jet with lighter spheres (FPD98) and heavier spheres (FPA97)

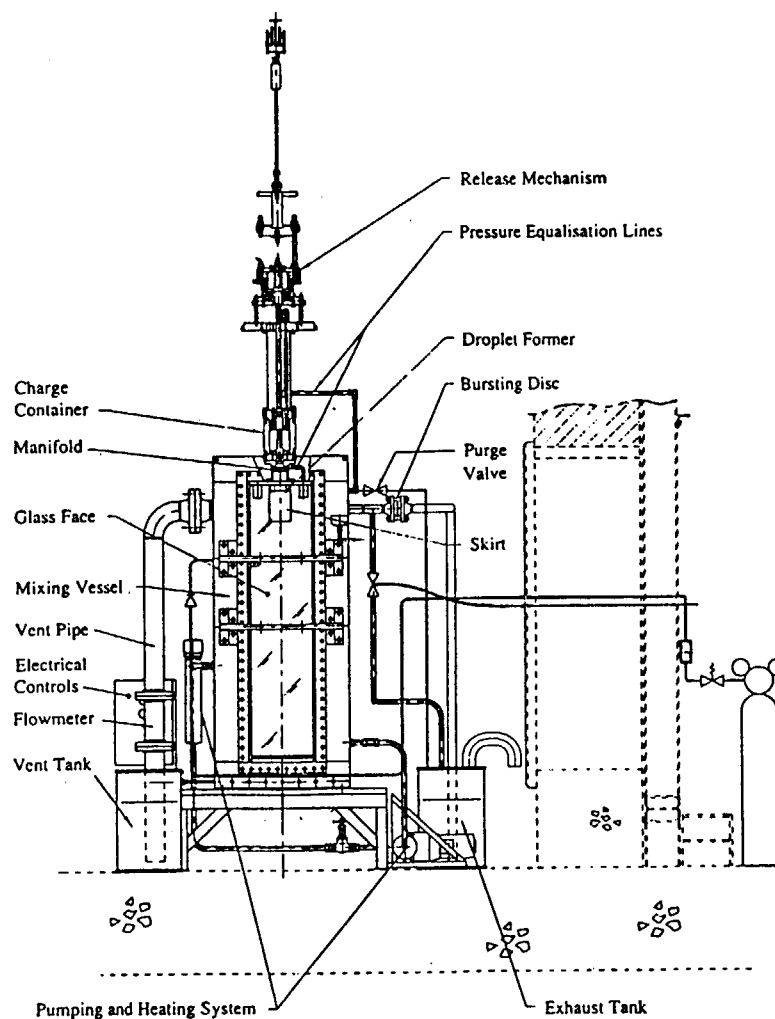


Figure 6 MIXA experimental setup

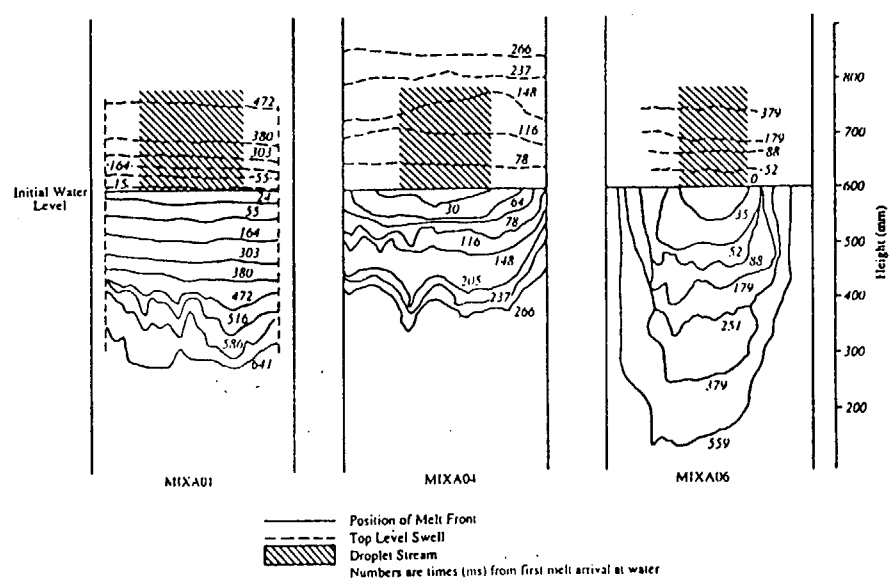


Figure 7 MIXA experiment: Melt front locations and water level swell of three tests

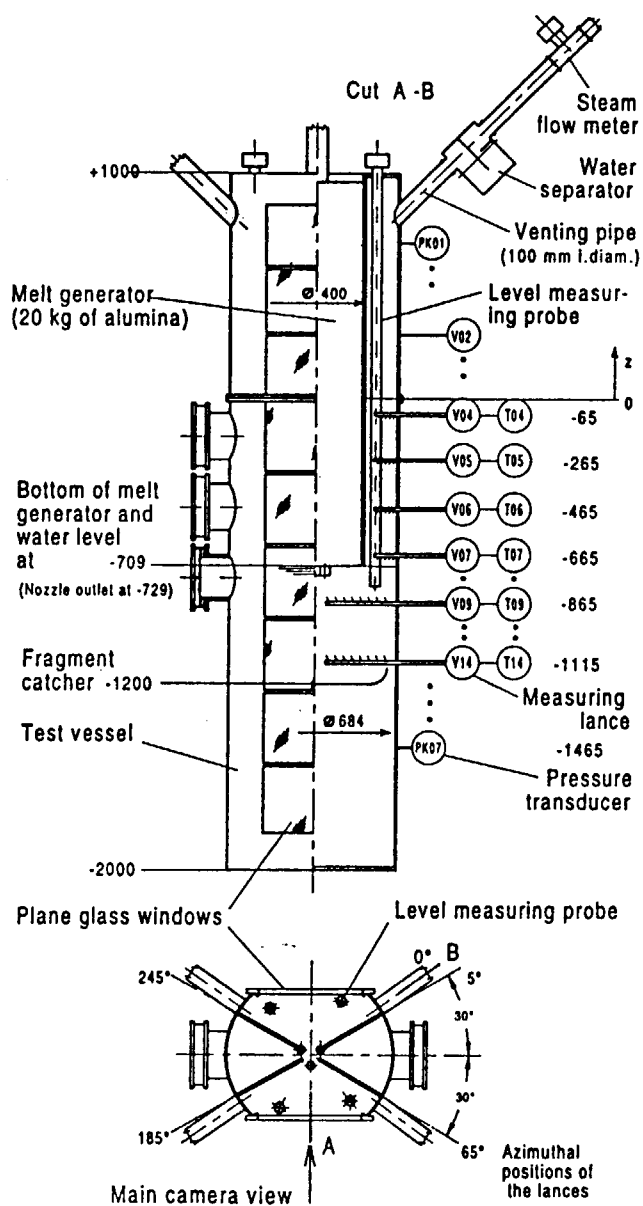


Figure 8 PREMIX test facility

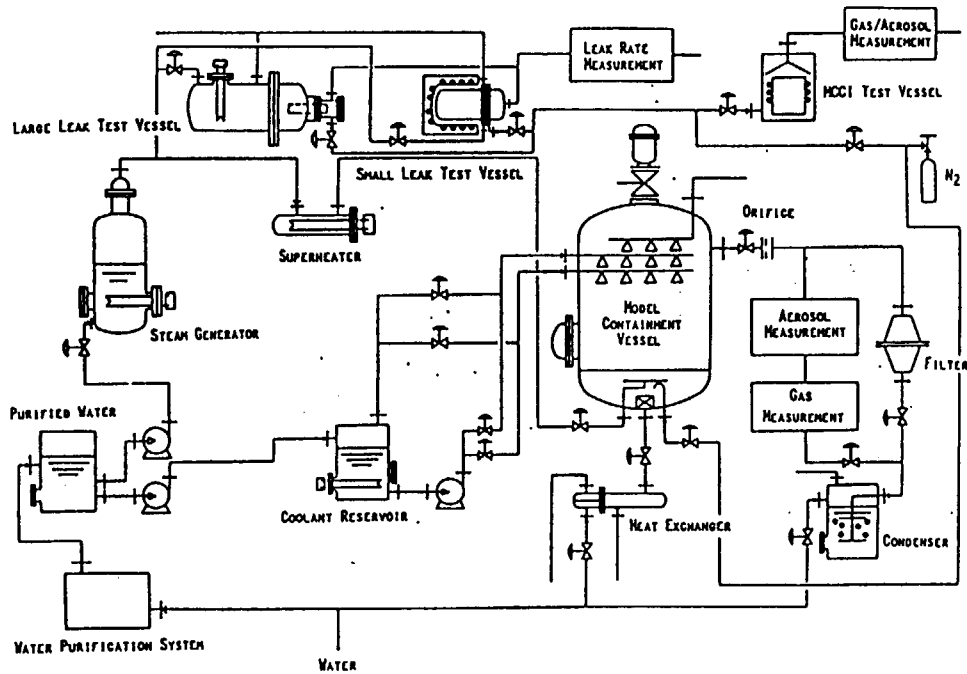


Figure 9 Diagram of ALPHA test Facility

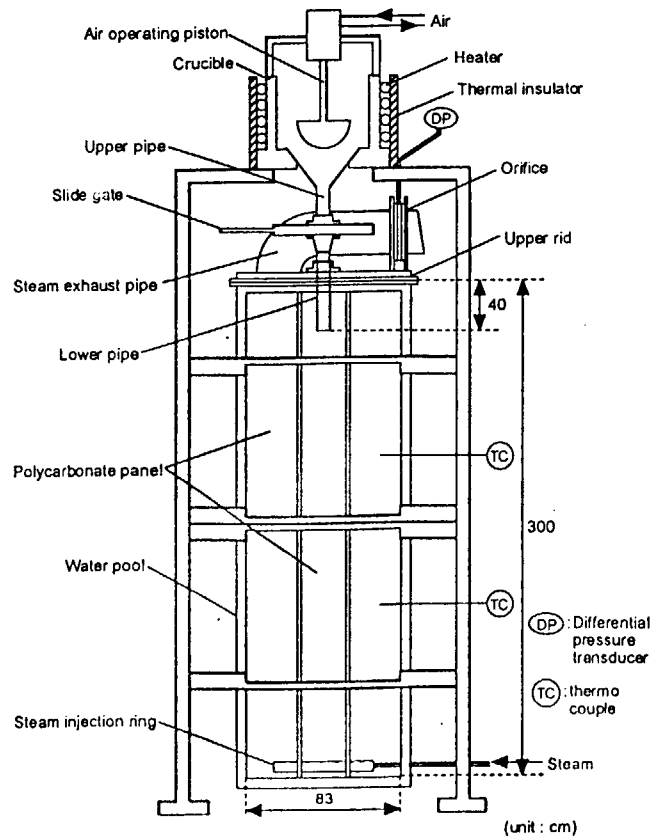


Figure 10 Conceptual diagram of ALPHA-MJB test equipment

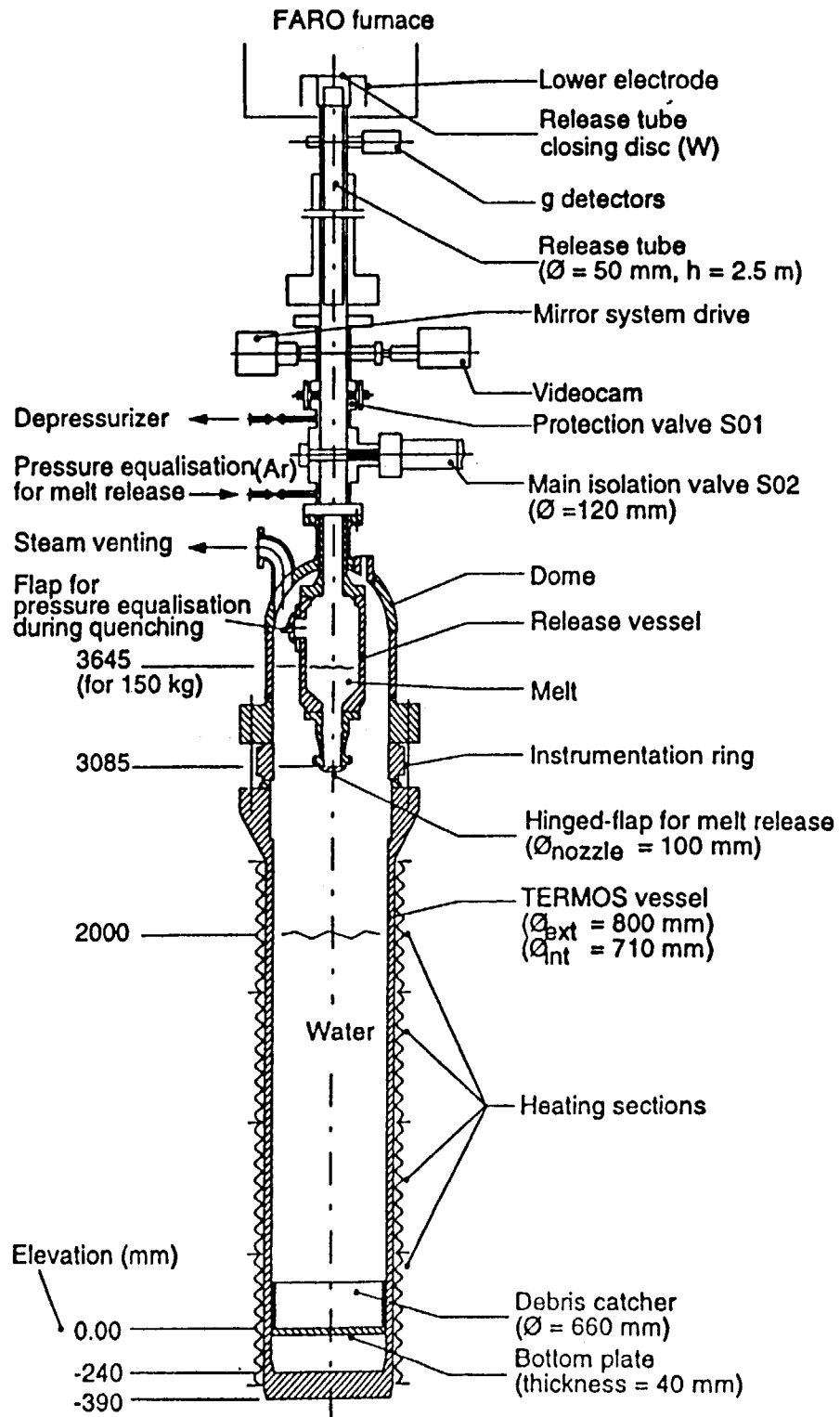


Figure 11 FARO experimental facility

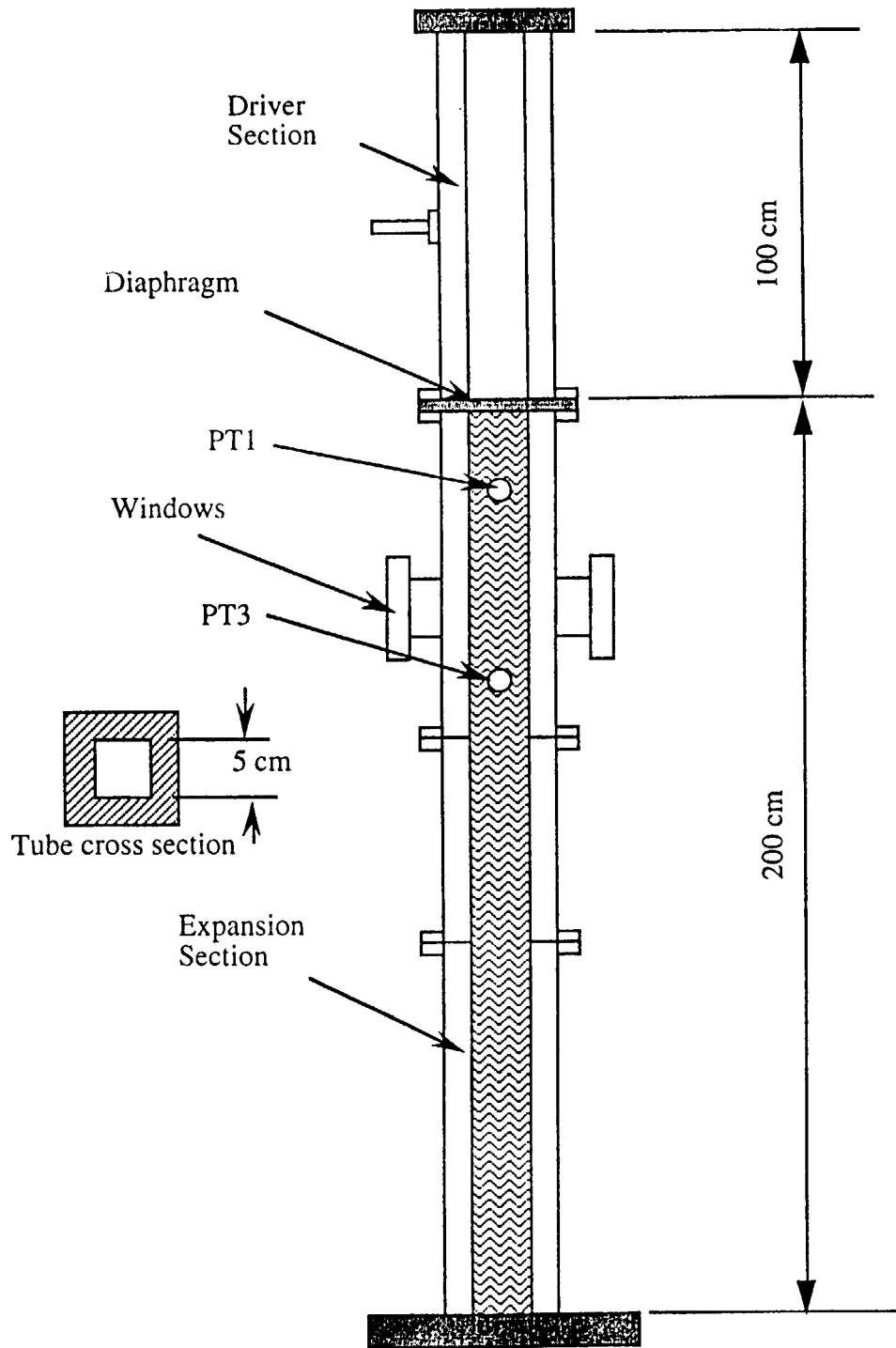


Figure 12 Schema of SIGMA-2000 test setup

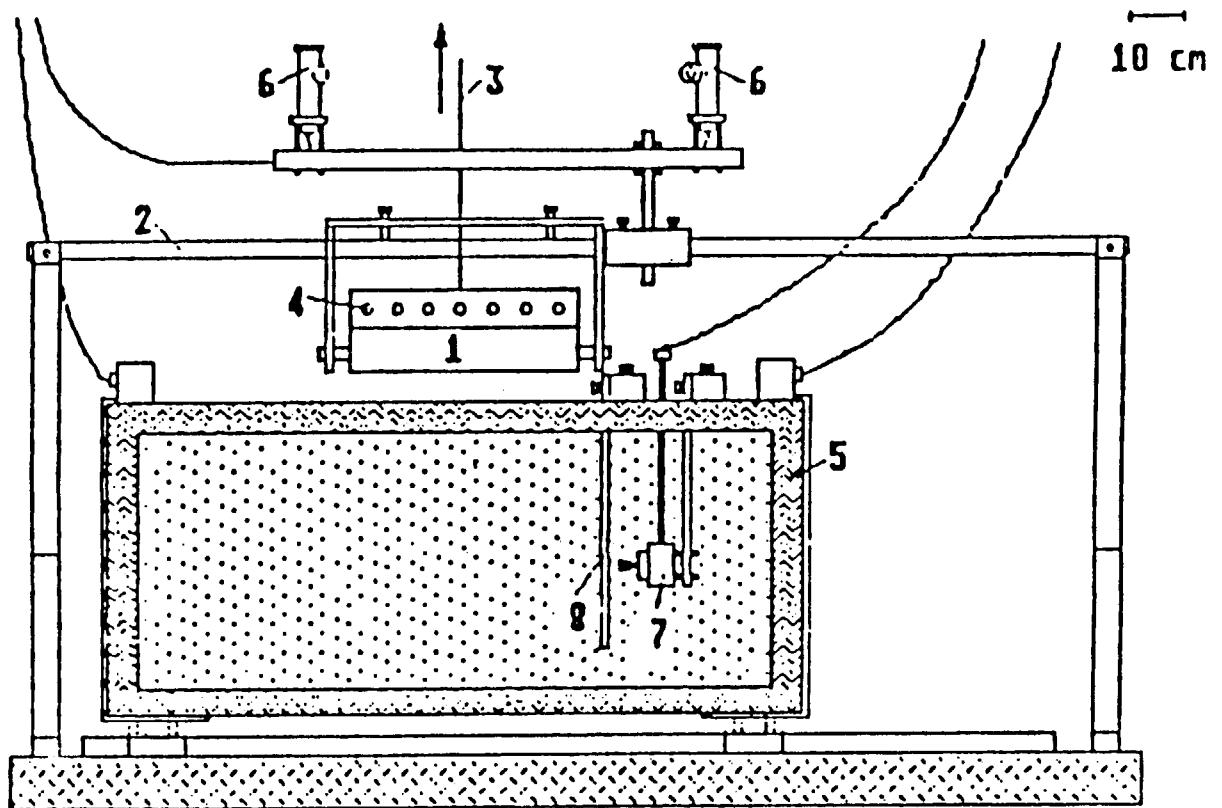


Figure 13 Front view of IKE MULTI-JET test facility

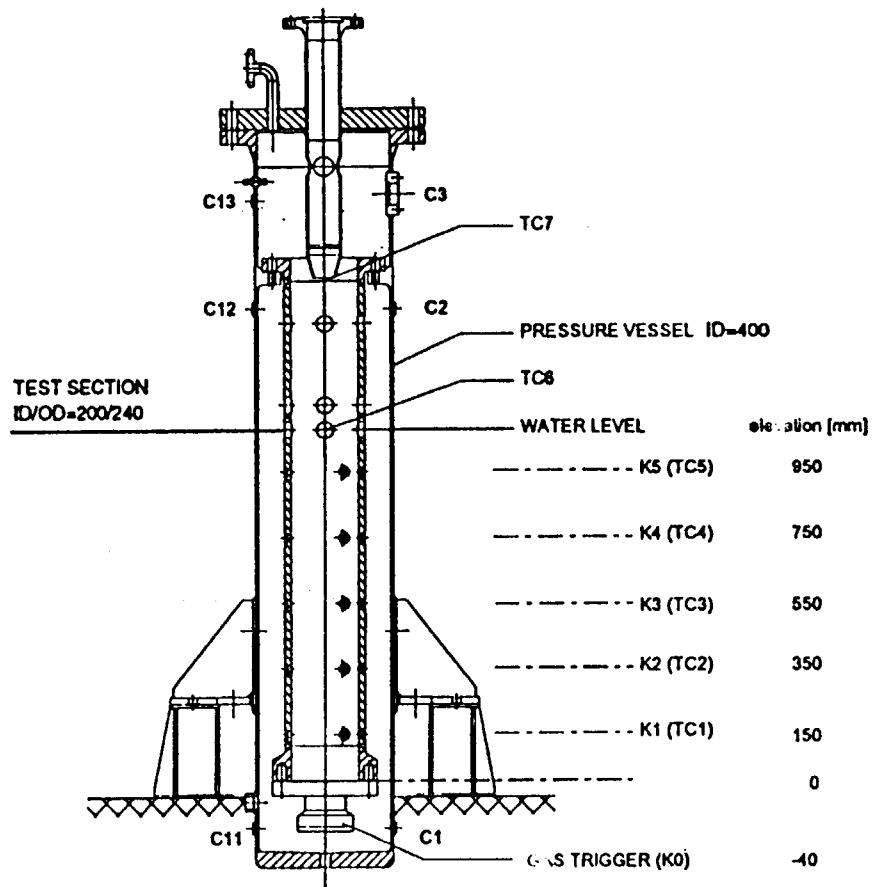


Figure 14 KROTOS test section

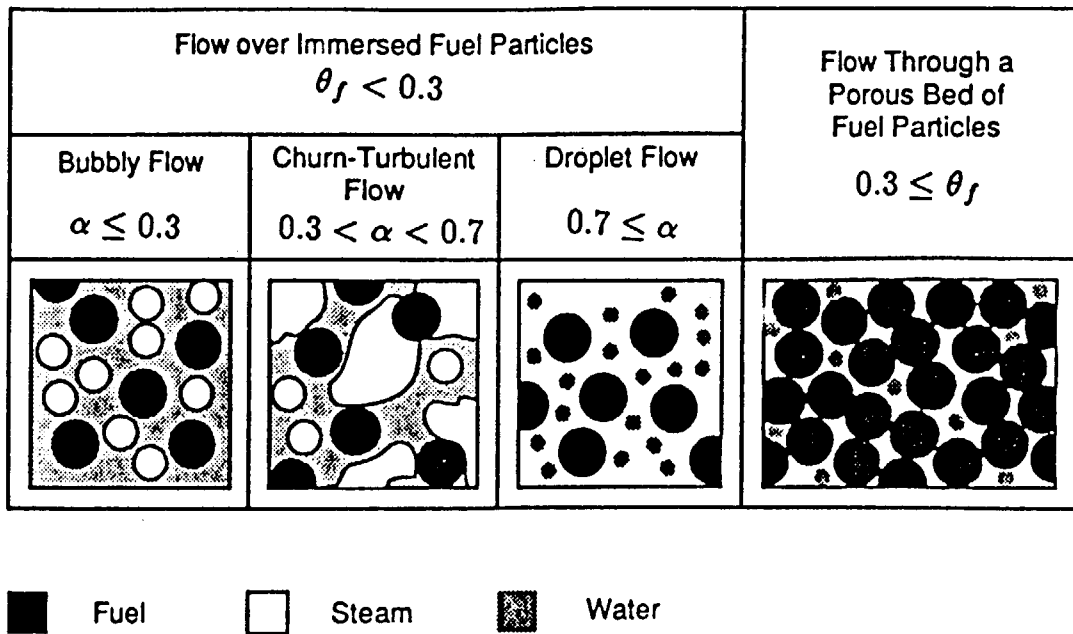


Figure 15 Flow regime map used in PM-ALPHA code

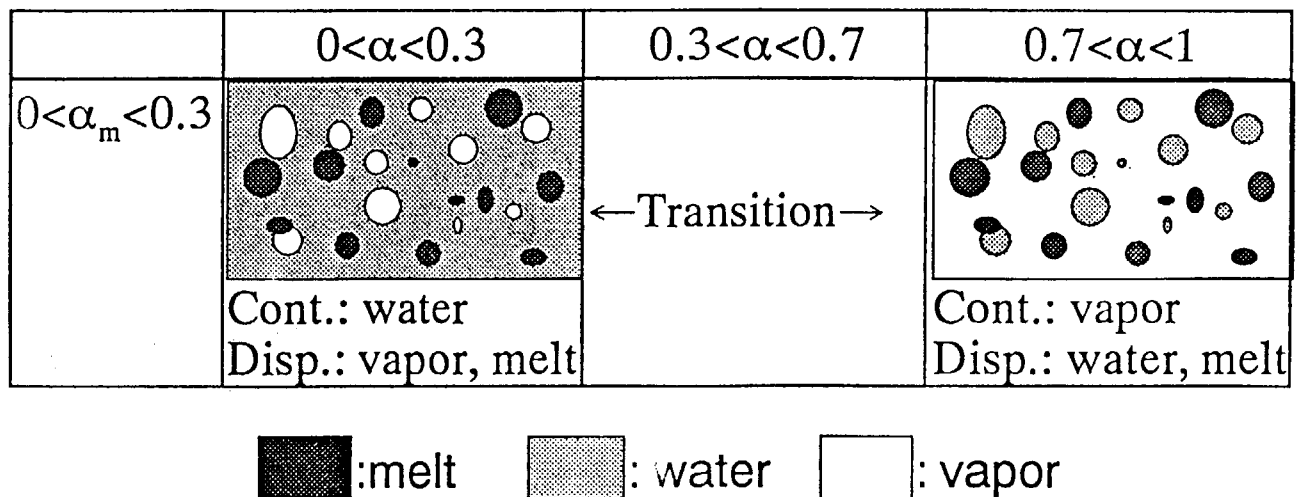


Figure 16 Flow regime map used in JASMINE code

国際単位系 (SI) と換算表

表1 SI基本単位および補助単位

量	名称	記号
長さ	メートル	m
質量	キログラム	kg
時間	秒	s
電流	アンペア	A
熱力学温度	ケルビン	K
物質	モル	mol
光	カンデラ	cd
平面角	ラジアン	rad
立体角	ステラジアン	sr

表3 固有の名称をもつ SI組立単位

量	名称	記号	他の SI 単位 による表現
周波数	ヘルツ	Hz	s ⁻¹
力	ニュートン	N	m·kg/s ²
圧力, 応力	パスカル	Pa	N/m ²
エネルギー, 仕事, 熱量	ジュール	J	N·m
工率, 放射束	ワット	W	J/s
電気量, 電荷	クーロン	C	A·s
電位, 電圧, 起電力	ボルト	V	W/A
静電容量	ファラド	F	C/V
電気抵抗	オーム	Ω	V/A
コンダクタンス	ジーメン	S	A/V
磁束	ウェーバ	Wb	V·s
磁束密度	テスラ	T	Wb/m ²
インダクタンス	ヘンリー	H	Wb/A
セルシウス温度	セルシウス度	°C	
光束	ルーメン	lm	cd·sr
照度	ルクス	lx	lm/m ²
放射能	ベクレル	Bq	s ⁻¹
吸収線量	グレイ	Gy	J/kg
線量当量	シーベルト	Sv	J/kg

表2 SIと併用される単位

名称	記号
分, 時, 日	min, h, d
度, 分, 秒	°, ', "
リットル	l, L
トン	t
電子ボルト	eV
原子質量単位	u

$$1 \text{ eV} = 1.60218 \times 10^{-19} \text{ J}$$

$$1 \text{ u} = 1.66054 \times 10^{-27} \text{ kg}$$

表4 SIと共に暫定的に維持される単位

名称	記号
オングストローム	Å
バーン	b
バル	bar
ガリ	Gal
キュリー	Ci
レントゲン	R
ラド	rad
レム	rem

$$1 \text{ Å} = 0.1 \text{ nm} = 10^{-10} \text{ m}$$

$$1 \text{ b} = 100 \text{ fm}^2 = 10^{-28} \text{ m}^2$$

$$1 \text{ bar} = 0.1 \text{ MPa} = 10^5 \text{ Pa}$$

$$1 \text{ Gal} = 1 \text{ cm/s}^2 = 10^{-2} \text{ m/s}^2$$

$$1 \text{ Ci} = 3.7 \times 10^{10} \text{ Bq}$$

$$1 \text{ R} = 2.58 \times 10^{-4} \text{ C/kg}$$

$$1 \text{ rad} = 1 \text{ cGy} = 10^{-2} \text{ Gy}$$

$$1 \text{ rem} = 1 \text{ cSv} = 10^{-2} \text{ Sv}$$

表5 SI接頭語

倍数	接頭語	記号
10 ¹⁸	エクサ	E
10 ¹⁵	ペタ	P
10 ¹²	テラ	T
10 ⁹	ギガ	G
10 ⁶	メガ	M
10 ³	キロ	k
10 ²	ヘクト	h
10 ¹	デカ	da
10 ⁻¹	デシ	d
10 ⁻²	センチ	c
10 ⁻³	ミリ	m
10 ⁻⁶	マイクロ	μ
10 ⁻⁹	ナノ	n
10 ⁻¹²	ピコ	p
10 ⁻¹⁵	フェムト	f
10 ⁻¹⁸	アト	a

(注)

- 表1～5は「国際単位系」第5版, 国際度量衡局 1985年刊行による。ただし, 1 eV および 1 uの値は CODATA の1986年推奨値によった。
- 表4には海里, ノット, アール, ヘクタールも含まれているが日常の単位なのでここでは省略した。
- barは, JISでは流体の圧力を表わす場合に限り表2のカテゴリーに分類されている。
- EC閣僚理事会指令では bar, barn および「血圧の単位」 mmHg を表2のカテゴリーに入れている。

換算表

力	N (=10 ⁵ dyn)	kgf	lbf
	1	0.101972	0.224809
	9.80665	1	2.20462
	4.44822	0.453592	1

$$\text{粘度 } 1 \text{ Pa} \cdot \text{s} (\text{N} \cdot \text{s/m}^2) = 10 \text{ P (ポアズ)} (\text{g}/(\text{cm} \cdot \text{s}))$$

$$\text{動粘度 } 1 \text{ m}^2/\text{s} = 10^4 \text{ St (ストークス)} (\text{cm}^2/\text{s})$$

圧	MPa (=10 bar)	kgf/cm ²	atm	mmHg (Torr)	lbf/in ² (psi)
	1	10.1972	9.86923	750062 × 10 ³	145.038
力	0.0980665	1	0.967841	735.559	14.2233
	0.101325	1.03323	1	760	14.6959
	1.33322 × 10 ⁻⁴	1.35951 × 10 ⁻³	1.31579 × 10 ⁻³	1	1.93368 × 10 ⁻²
	6.89476 × 10 ⁻³	7.03070 × 10 ⁻²	6.80460 × 10 ⁻²	51.7149	1

エネルギー・仕事・熱量	J (=10 ⁷ erg)	kgf·m	kW·h	cal (計量法)	Btu	ft·lbf	eV
	1	0.101972	2.77778 × 10 ⁻⁷	0.238889	9.47813 × 10 ⁻⁴	0.737562	6.24150 × 10 ¹⁸
	9.80665	1	2.72407 × 10 ⁻⁶	2.34270	9.29487 × 10 ⁻³	7.23301	6.12082 × 10 ¹⁹
	3.6 × 10 ⁶	3.67098 × 10 ⁵	1	8.59999 × 10 ⁵	3412.13	2.65522 × 10 ⁶	2.24694 × 10 ²⁵
	4.18605	0.426858	1.16279 × 10 ⁻⁶	1	3.96759 × 10 ⁻³	3.08747	2.61272 × 10 ¹⁹
	1055.06	107.586	2.93072 × 10 ⁻⁴	252.042	1	778.172	6.58515 × 10 ²¹
	1.35582	0.138255	3.76616 × 10 ⁻⁷	0.323890	1.28506 × 10 ⁻³	1	8.46233 × 10 ¹⁸
	1.60218 × 10 ⁻¹⁹	1.63377 × 10 ⁻²⁰	4.45050 × 10 ⁻²⁶	3.82743 × 10 ⁻²⁰	1.51857 × 10 ⁻²²	1.18171 × 10 ⁻¹⁹	1

$$1 \text{ cal} = 4.18605 \text{ J (計量法)}$$

$$= 4.184 \text{ J (熱化学)}$$

$$= 4.1855 \text{ J (15 °C)}$$

$$= 4.1868 \text{ J (国際蒸気表)}$$

$$\text{仕事率 } 1 \text{ PS (仏馬力)}$$

$$= 75 \text{ kgf} \cdot \text{m/s}$$

$$= 735.499 \text{ W}$$

放射能	Bq	Ci
	1	2.70270 × 10 ⁻¹¹
	3.7 × 10 ¹⁰	1

吸収線量	Gy	rad
	1	100
	0.01	1

照射線量	C/kg	R
	1	3876
	2.58 × 10 ⁻⁴	1

線量当量	Sv	rem
	1	100
	0.01	1

(86年12月26日現在)

THE PREMIXING AND PROPAGATION PHASES OF FUEL-COOLANT INTERACTIONS: A REVIEW OF RECENT EXPERIMENTAL STUDIES AND CODE DEVELOPMENTS